UHASSELT
KNOWLEDGE IN ACTION

Maastricht University

Faculteit Geneeskunde en Levenswetenschappen
School voor Levenswetenschappen

master in de biomedische wetenschappen

Masterthesis

Interleukin-13 secreting macrophages improve functional recovery after spinal cord injury by exerting M2 effects and secreting interleukin-13

Thibaut Goethuys

Scriptie ingediend tot het behalen van de graad van master in de biomedische wetenschappen, afstudeerrichting klinische moleculaire wetenschappen

PROMOTOR :

Prof. dr. Sven HENDRIX

dr. Stefanie LEMMENS

BEGELEIDER :

Mevrouw Jana VAN BROECKHOVEN

2018
2019

De transnationale Universiteit Limburg is een uniek samenwerkingsverband van twee universiteiten in twee landen: de Universiteit Hasselt en Maastricht University.

UHASSELT
KNOWLEDGE IN ACTION

www.uhasselt.be
Universiteit Hasselt
Campus Hasselt:
Martelarenlaan 42 | 3500 Hasselt
Campus Diepenbeek:
Agoralaan Gebouw D | 3590 Diepenbeek

UHASSELT
KNOWLEDGE IN ACTION

Maastricht University

Faculteit Geneeskunde en Levenswetenschappen

School voor Levenswetenschappen

master in de biomedische wetenschappen

Masterthesis

Interleukin-13 secreting macrophages improve functional recovery after spinal cord injury by exerting M2 effects and secreting interleukin-13

Thibaut Goethuys

Scriptie ingediend tot het behalen van de graad van master in de biomedische wetenschappen, afstudeerrichting klinische moleculaire wetenschappen

PROMOTOR :

Prof. dr. Sven HENDRIX

dr. Stefanie LEMMENS

BEGELEIDER :

Mevrouw Jana VAN BROECKHOVEN

> ***What makes spinal cord injuries as devastating as they are is that everything about them plays out in absolutes: they are instantaneous, utterly disabling, and horribly permanent*** *- Jeffrey Kluger (American writer)*

Table of contents

Acknowledgements

Every story has an end and so has this one. My senior internship adventure has almost finished and so, my time of being a student is almost over. It was not always an easy road, but luckily I did not have to walk it alone. Many people stood by my side and I was not able to finish it if they were not there for me. Therefore, I would like to thank everyone who supported me and helped me during my studies and senior internship.

First of all, I would like to thank Prof. Dr. Sven Hendrix for giving me the opportunity to join his research group and allowing me to be part of this beautiful research project. Furthermore, my appreciation goes out to Prof. Dr. Sven Hendrix and Dr. Stefanie Lemmens for providing me the sufficient amount of knowledge within their research field. As this was crucial in finishing this thesis. I am very grateful to them for teaching me how to have a critical view on research and to think about all the aspects involved in fundamental research. I learned many things during the various lab meetings. I learned that research is not only about conducting experiments, but mainly about thinking and being critical. This knowledge was not only helpful during my internship, but will also be necessary in the future. Therefore, I would like to thank them for the life-long knowledge I was allowed to gain.

Furthermore, I would like to thank my daily supervisor, Drs. Jana Van Broeckhoven for her daily guidance, support, and trust. I am very pleased to have been part of her research and to have learned many skills during this period. Even when experiments were not always going well, she was supportive and taught me to push my boundaries. I wish her the best during the remainder of her doctorate and many wonderful results in the near future.

Furthermore, my appreciation goes out to every member of the morphology research group, namely Céline Erens, Selien Sanchez, Dr. Daniela Sommer, and Dr. Leen Timmermans for the warm welcome and always supporting me, both inside and outside the lab. I achieved many skills and much knowledge from each group member, for which I am very grateful. I would also like to thank my second examiner, Prof. Dr. Bert Brône, for the helpful feedback, tips and his interest in the project.

Moreover, I am grateful for the wonderful conversations with my fellow students and for always being there for each other, even during the difficult periods. I will always remember the coffee breaks full of joy and laughter.
I would also like to thank my parents and family members for supporting me and always encouraged me to keep fighting and pursuing my dreams. For teaching me that life is not always an easy game to play and that, whatever happens, you will always have someone to fall back on. Finally, last but definitely not least, I would like to thank Leen, as she was always there for me. Even when things did not work out the way I wanted, she stood by my side and supported me. Whenever I fell, she was there to catch me and she always lend an ear when I needed one. I will always remember that the most unexpected things in life are sometimes the most beautiful.

Thibaut Goethuys

List of abbreviations

Arg-1 Arginase-1

BMDM Bone marrow-derived macrophages

BMS Basso mouse scale

CD Cluster of differentiation

cDNA Complement DNA

CM Conditioned medium

CNS Central nervous system

CycA Cyclin A

DAPI 4' ,6-diamidino-2-phenylindole

dpi Days post injury

DMEM Dulbecco's Modified Eagle's Medium

ELISA Enzyme-linked immunosorbent assay

Fizz Resistin like alpha

GAPDH Glyceraldehyde 3-phosphate dehydrogenase

hiFCS heat-inactivated fetal calf serum

HMBS Hydroxymethylbilane synthase

IL Interleukin

IL-4R Interleukin-4 receptor

iNOS Inducible nitric oxide synthase

KO Knockout

LCM L929 conditioned medium

LPS Lipopolysacharide

LV Lentiviral vectors

Mφs Macrophages

MBP Myelin basic protein

MHC-II Major histocompatibility complex class II

mRNA Messenger RNA

MSC Mesenchymal stem cell

pSTAT Phosphorylated signal transducer and activator of transcription

PBS Phosphate-buffered saline

PFA Paraformaldehyde

P/S Penicillin/Streptomycin

PVDF Polyvinylidene fluoride

qPCR Quantitative polymerase chain reaction

RIPA Radioimmunoprecipitation assa

SCI Spinal cord injury

SDF-1 Stromal cell-derived factor-1

SDS Sodium dodecyl sulfate

SEM Standard error of the mean

STAT Signal transducer and activator of transcription

TBS-T Tris-buffered saline – Tween 2

TNFα Tumor necrosis factor alpha

WT Wild type

Ym1 Chitinase 3-like 3

YWHAZ 14-3-3 protein zeta/delta

5-HT Serotonin

Summary

Introduction: Spinal cord injury (SCI) is a severe condition that has an enormous impact on society. In Europe, approximately 250 people per million inhabitants suffer from SCI. No effective therapy is available for these patients and current treatment options merely focus on symptom relieve. One of the main hallmarks of SCI is the chronic neuroinflammation, contributing to immune-related neural damage and limiting spinal cord repair. The key players involved in this inflammatory event are macrophages, being extensively present within the lesion epicenter. These macrophages are mainly present in a pro-inflammatory state. This will consequently aggravate neuroinflammation and prevent initial repair processes. Multiple studies show that shifting these macrophages towards an anti-inflammatory state, ameliorates the condition. Moreover, interleukin-13 (IL-13), an M2 macrophage-related cytokine, protects neurons and stimulates neural repair. Within this research, we combine the positive effects of both M2 macrophages and IL-13 by creating IL-13 secreting macrophages. Accordingly, we hypothesized that IL-13 secreting macrophages improve functional recovery after SCI by locally exerting M2 functions and secreting IL-13.

Material and methods: Murine-obtained bone marrow-derived macrophages were transduced with a lentiviral vector containing murine IL-13 cDNA. Firstly, we investigated the phenotype of the IL-13 macrophages by means of qPCR, western blot and ELISA. Additionally, we assessed their phenotypic properties under pro-inflammatory conditions with qPCR and western blot. Furthermore, the therapeutic potential of the IL-13 macrophages was evaluated in a dorsal T-cut hemisection mouse model by using the Basso mouse scale (BMS). The significance of IL-13 signaling in functional recovery was investigated in an IL-4 receptor knockout mouse model. Moreover, the migratory ability of IL-13 macrophages was assessed by means of a Boyden chamber assay and *in vivo* tracking of these macrophages in SCI mice. The effect of IL-13 macrophages on the pro-inflammatory environment of the injured spinal cord was investigated by using qPCR.

Results: IL-13 macrophages showed expression of anti-inflammatory markers (e.g. Arginase-1, Fizz, CD206, and Ym1) and secretion of IL-13. Expression of these markers was also observed under pro-inflammatory conditions. Furthermore, the IL-13 macrophages induced anti-inflammatory characteristics in M1 macrophages. Importantly, transplantation of IL-13 macrophages significantly improved functional recovery after SCI. This improvement was due to the activation of IL-13 signaling pathways. Yet, migration of these cells was not observed at seven days post injury. Additionally, IL-13 macrophages had no effect on the pro-inflammatory environment of the injured spinal cord.

Conclusion: IL-13 macrophages show an anti-inflammatory macrophage phenotype, even under pro-inflammatory conditions. Importantly, these cells improve functional recovery after SCI by the induction of IL-13 signaling pathways. Migration and anti-inflammatory effects were not observed within seven days after SCI. However migratory, neuro-protective and –regenerative properties have yet to be investigated.

Samenvatting

Introductie: Ruggenmergletsel is een ernstige aandoening die een enorme impact heeft op de maatschappij. In Europa lijden ongeveer 250 personen per miljoen inwoners aan een dwarslaesie. Momenteel is er geen effectieve behandeling voor deze aandoening en ligt de focus voornamelijk op het aanpakken van symptomen. Één van de kenmerken van een dwarslaesie is het optreden van chronische neuro-inflammatie, die bijdraagt aan immuun-gerelateerde neurale schade en die herstel hindert. De hoofdrolspelers binnen dit inflammatoir proces zijn macrofagen. Deze cellen zijn namelijk sterk aanwezig binnen de laesie. De macrofagen hebben een pro-inflammatoir fenotype, waardoor neuro-inflammatie gestimuleerd wordt en herstel belemmerd wordt. Verschillende studies tonen aan dat het verschuiven van het macrofaag fenotype naar een anti-inflammatoire staat, de conditie verbetert. Bovendien is aangetoond dat interleukine-13 (IL-13), een M2 macrofaag-gerelateerd cytokine, neuronen beschermd en neuraal herstel bevordert. Binnen dit onderzoek combineren we de positieve effecten van M2 macrofagen met deze van IL-13 door het creëren van macrofagen die IL-13 secreteren. Bij deze veronderstellen we dat IL-13 macrofagen functioneel herstel na een dwarslaesie verbeteren door lokaal M2 functies uit te oefenen en IL-13 te secreteren.

Materiaal en methoden: Macrofagen werden getransduceerd met een lentivirale vector met IL-13 cDNA. Het fenotype van de IL-13 macrofagen werd onderzocht via qPCR, western blot en ELISA. Bijkomend werden de fenotypische kenmerken van deze cellen, onder pro-inflammatoire condities, bestudeerd met behulp van qPCR en western blot. Verder werd het potentieel van de IL-13 macrofagen onderzocht in een dwarslaesie muis model door gebruik van de Basso mouse scale. De invloed van IL-13 signalisatie in functioneel herstel werd bestudeerd in een IL-4 receptor knockout model. Bijkomend werd de migratie van de IL-13 macrofagen onderzocht met behulp van een Boyden chamber assay en het *in vivo* traceren van deze cellen in een SCI muis model. Het effect van de macrofagen op de pro-inflammatoire conditie van het beschadigd ruggenmerg werd onderzocht via qPCR.

Resultaten: De IL-13 macrofagen vertoonden expressie van anti-inflammatoire merkers (Arginase-1, Fizz, CD206 en Ym1) en secretie van IL-13. Expressie van deze merkers was tevens nog steeds zichtbaar onder pro-inflammatoire omstandigheden. Bijkomend werd aangetoond dat IL-13 macrofagen anti-inflammatoire eigenschappen konden induceren in M1 macrofagen. Transplantatie van deze cellen induceerde een significante verbetering in het functioneel herstel na een dwarslaesie. Deze verbetering was te wijten aan IL-13 signalisatie. Echter, migratie van de cellen werd niet aangetoond op de zevende dag na de dwarslaesie. Tevens hadden de cellen geen effect op de pro-inflammatoire omgeving van het ruggenmerg.

Conclusie: IL-13 macrofagen hebben een anti-inflammatoir fenotype, tevens onder pro-inflammatoire condities. Belangrijk, deze cellen verbeteren functioneel herstel na een dwarslaesie door het induceren van IL-13 signalisatie. Migratie en anti-inflammatoire effecten van de cellen kon niet worden aangetoond op zeven dagen na dwarslaesie. Echter dienen de migratie, neuro-protectieve, en -regeneratieve eigenschappen van deze cellen nog verder onderzocht te worden.

1 Introduction

1.1 Spinal cord injury

Spinal cord injury (SCI) is a devastating neurological disorder of the central nervous system (CNS). Worldwide, every year, SCI affects between 3.6 and 195.4 people per million inhabitants (1). The estimated mean European prevalence is currently 250 cases per million inhabitants, but is believed to increase in the near future. Reflected to the Belgian population, this indicates that approximately 2,850 people suffer from a SCI (4). The etiology of this severe functional loss is either of traumatic or non-traumatic origin. The former is caused when an external force acutely injures the spinal cord (e.g. a motor vehicle accident, violence, or a fall) while the latter is caused by an internal source, acutely or chronically damaging the spinal cord's neural networks (e.g. tumor compression, infection or blood supply loss) (2). Consequences of this condition include life-long sensorimotor deficits, autonomic dysfunction and patients require continuous physical support, all reducing quality of life of these patients (3-6). In addition, the estimated lifetime economic burden of SCI patients is estimated to range from 1.5 to 3.0 million dollars (7, 8). Therefore, SCI has a profound impact on both society and the healthcare system.

Unfortunately, to date, no cure for SCI is available. Current therapeutic options include 1) spinal cord decompression, 2) administration of anti-inflammatory reagents (e.g. methylprednisolone) and 3) functional rehabilitation (9). These interventions have shown to be successful in symptom relief and stabilizing the condition. However, they have failed to show significant axonal repair (10, 11). In contrast, several experimental approaches (e.g. the use of stem cells) show promising results, although the translation to the clinic is rather poor with only limited successful cases (12). Therefore, new innovative therapeutic approaches for SCI are yet to be established.

1.2 Pathogenesis of spinal cord injury

The pathogenesis of SCI consists of two distinct phases. The primer phase consists of the structural damage caused by the mechanical disruption of the spinal cord. This directly results in damaged neurons, myelin sheets, and the surrounding vasculature. This initial damage disrupts the structural and functional properties of the spinal cord. Consequently, the primary injury immediately results in sensorimotor deficits, immobility and pain (13). Furthermore, all the local events result in a chaotic micro-environment, dominated by extensive cell death and the accumulation of cytotoxic substances. Following these injurious effects, structural and cellular changes will take place. These events further damage the traumatic area and worsen the condition. In summary, damage to neurons and additional structures results in the release of cellular and cytotoxic substances, leading to neurotransmitter excitotoxicity, immune cell infiltration, and vascular injury (14, 15). Collectively, these extensive molecular alterations are part of a secondary injury cascade which aggravates the initial damage. The secondary phase begins within minutes after the injury and can persist for weeks or months (16). Several secondary injury mechanisms are present within the spinal cord. For instance, the accumulation of free radicals and neurotransmitters results in lipid peroxidation and excitotoxicity, respectively. These events lead to the damage of multiple CNS cell types. Furthermore, after SCI, an immune response is elicited and

leukocytes are activated and start infiltrating at the site of injury, including neutrophils, lymphocytes and macrophages (17-20). These immune cells secrete pro-inflammatory cytokines, creating an extensive hostile environment (21). This inflammatory event can damage healthy tissue, thereby exacerbating the initial injury (22). Due to a combination of primary and secondary injury mechanisms, demyelination is also distinct within the lesion site (23). This demyelination can be explained by the loss of oligodendrocytes, making neurons more susceptible to the cytotoxic effect of cytokines and free radicals. In addition, the loss of myelin results in conduction delays and even conduction deficits (24). Extensive activation of astrocytes, also defined as astrogliosis, occurs within the injured spinal cord (25, 26). This event aims at limiting tissue damage and restoring homeostasis (27). However, in case of severe injury, astrogliosis inhibits the neural plasticity which is crucial for CNS tissue regeneration, thereby limiting functional recovery (28, 29). As all these events gradually damage neural tissue, the lesion progresses to a chronic phase which is characterized by the formation of cystic cavities and glial scar formation. These formed cavities, together with the distinct glial scarring, serves as a structural barrier for neural repair and remyelination (30). This occurrence limits the regenerative potential of the spinal cord and restricts long-term functional improvement. These events, in combination with the poor regenerative ability of the CNS, makes SCI a permanently disabling disorder with enduring neural deficits (2, 31).
The primary injury to the spinal cord can not be prevented. Nevertheless, the secondary injury mechanisms, which further damage the traumatic area and limit recovery, can be restricted. Therefore, it is utterly important to prevent the occurrence of these molecular and cellular events and diminish the extent of secondary injury caused to the spinal cord.

1.3 Chronic inflammatory response

After SCI, a chronic inflammatory response occurs within the spinal cord. This is defined as neuroinflammation and is one of the main hallmarks of SCI. This event is characterized by the activation of resident glia (i.e. microglia and astrocytes), the influx of blood-borne immune cells (e.g. monocytes), as well as the production of pro-inflammatory cytokines, chemokines and reactive oxygen species within the injured spinal cord (figure 1) (20, 32, 33). Moreover, the neuroinflammatory response is evident within minutes after injury and can persist up to months or even years after the initial insult (34). Leukocytes infiltrate the spinal cord after injury, including neutrophils, lymphocytes and macrophages. The latter is a key player in the response to SCI. Macrophages become activated upon injury and start migrating towards the lesion epicenter within a day after SCI. These cells migrate towards chemokines present within the lesion (35). For instance, a potent chemokine in case of SCI is stromal cell-derived factor-1 (SDF-1). This chemokine is expressed in the injured spinal cord and has a substantial role in the attraction of macrophages (36). Moreover, inhibition of cell migration significantly reduces the amount of macrophages within the lesion epicenter, thereby showing the importance of migration in cell response after SCI (37). All the involved cell types are responsible for the detrimental immune response following SCI (34). Both beneficial and detrimental effects can be ascribed to this inflammatory event (38, 39). More specific, the infiltration of immune cells within the lesion site is essential for cellular and myelin debris removal. This removal is crucial for the initiation of tissue repair (40). In contrast, the accumulation of leukocytes can cause damage to the spinal cord via

the production of cytotoxic molecules. This includes the secretion of reactive metabolites and pro-inflammatory cytokines. This harmful effect results in an increased rate of apoptotic and necrotic cell death (41). In case of a persistent inflammatory response, the induced cell death significantly deteriorates the condition and limits endogenous repair of the CNS (41). Due to this chronic inflammatory event, functional recovery is limited and regeneration of the spinal cord is absent. Therefore, addressing neuroinflammation is an interesting concept in treating SCI, as it limits immune-related damage and alleviates the barrier of neuroregeneration. Accordingly, therapeutic approaches influencing this state of neuroinflammation are a promising intervention to improve functional recovery after SCI.

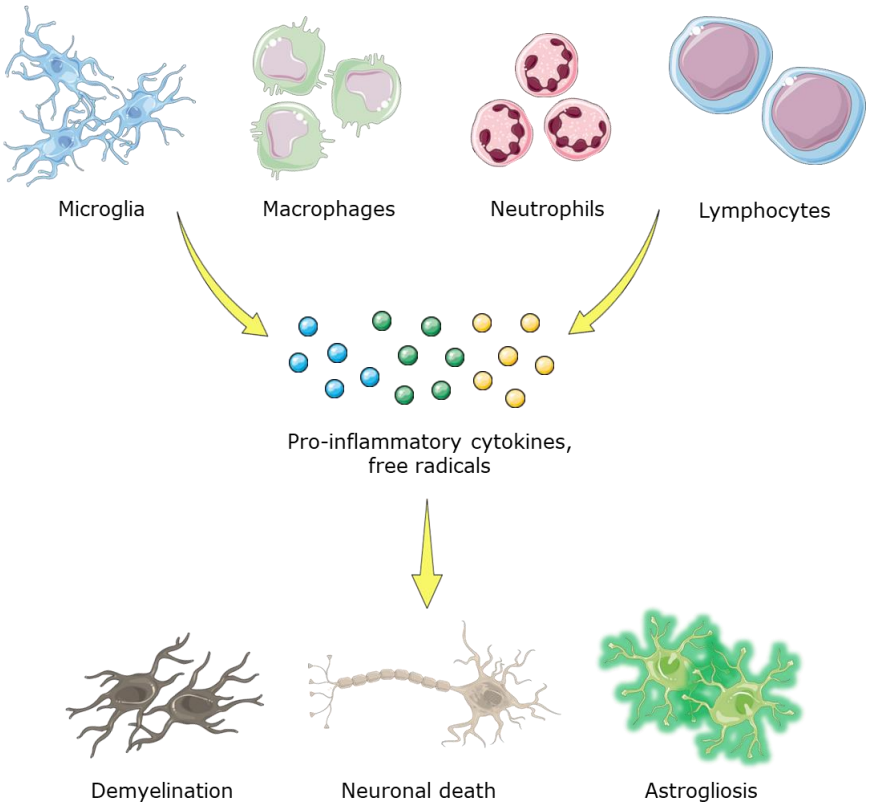

Figure 1: Neuroinflammation following spinal cord injury. Within seconds after SCI, an immune response is evoked, characterized by the activation of resident (i.e. microglia) and peripheral immune cells (i.e. macrophages, neutrophils, and lymphocytes). The multiple cell types produce and secrete pro-inflammatory cytokines and free radicals. These molecules are essential for efficient debris removal and tissue regeneration. However, in the case of SCI, a persistent inflammatory response is evident and results in demyelination (oligodendrocyte cell loss), neuronal death, and astrogliosis.

1.4 The role of macrophages in neuroinflammation

One of the main cell types involved in the neuroinflammatory response are the monocyte-derived macrophages (42). Macrophages (Mφs) have various physiological roles that are essential for tissue homeostasis, host defense and wound healing. In case of SCI, Mφs are considered to be the main contributor of the secondary injury cascade (22). Indeed, Mφ cell numbers significantly exceed those of other immune cells during the entire neuroinflammatory response. Maximum Mφ infiltration is observed at the 7th day post injury (dpi) and remains highly persistent throughout the complete course of the disease (17). For example, *Prüss et al.* demonstrated this enduring Mφ persistence, since 50% of the maximum Mφ cell number was still present within the injured spinal

cord at 55dpi. This finding indicates the relevance of this cell type within SCI (43). Due to their high presence within the lesion site, Mφs are key players during neuroinflammation and can positively or negatively affect functional recovery (44-46).

The role of Mφs in post-traumatic inflammation is controversial. Both beneficial and detrimental effects have been described in recent years (44, 47, 48). An explanation for these contradictory findings can be found in the various subsets of Mφs involved in inflammation. Based on the environment in which the Mφ is present, several cytokines determine the phenotype of this cell. These cytokines activate particular signaling cascades of the Mφ, resulting in the transcription of phenotype-related genes. The concerned cytokines can be pro-inflammatory, thereby activating signaling pathways which induce expression of pro-inflammatory genes. On the other hand, anti-inflammatory cytokines can stimulate the expression of anti-inflammatory genes. For simplicity reasons, Mφs can therefore be ascribed to either a pro-inflammatory (M1 Mφs) or anti-inflammatory profile (M2 Mφs) (49). M1 Mφs have been shown to contribute to immune-related injury to the CNS after SCI (50). Moreover, this injurious effect has been observed in various trauma-associated mouse models (48, 51). Due to the production of pro-inflammatory cytokines and cytotoxic by-products (e.g. free radicals), M1 Mφs exert detrimental effects on the surrounding neurons and oligodendrocytes. Importantly, various studies addressing this cytotoxic effect provided sufficient data to conclude that M1 Mφs hinder functional recovery and neural repair (50, 52). For example, *Popovich et al.* and *Gris et al.* demonstrated that depletion of M1 Mφs or neutralization of their by-products resulted in neuroprotection and an improved functional outcome in rats (53, 54). In contrast, anti-inflammatory M2 Mφs have the potential to stimulate tissue repair after SCI. In fact, this regenerative capacity can be ascribed to the production of anti-inflammatory cytokines, growth factors and neuroprotective molecules (18, 50). For example, various studies demonstrated that M2 Mφs are crucial for the restriction of immune-related damage and the improvement in recovery following SCI. *Ma et al.* showed that adoptive transfer of M2 Mφs stimulates functional recovery after SCI in rats. Furthermore, stimulation of M2 Mφ polarization and M2 Mφ-derived cytokine administration have all shown to be an effective approach to neural repair after trauma (55-57).

The described dichotomy in Mφ activation (i.e. M1/M2 Mφ activation) can firmly influence tissue repair. Under usual wound-healing conditions, sequential M1 and M2 Mφ activation properly initiates regeneration and remodeling of the injured tissue (58). In contrast, persistent M1 Mφ activation results in chronic inflammation and, consequently, impaired wound healing (59). This phenomenon is observed after SCI. A clear transition from M1 to M2 Mφs is absent and an excess of M1 Mφs remains visible for months or even years after the initial trauma (18). Consequently, a chronic pro-inflammatory state persists within the lesion site, exacerbating neuropathology and limiting CNS repair (47). Based on these data, addressing the sustained M1 Mφ activation after SCI is therefore an interesting approach to stimulate tissue regeneration and improve functional recovery.

As mentioned previously, current therapeutic interventions only address the symptoms after SCI (e.g. pain management) and barely focus on restoring function. Therefore, new approaches are necessary to effectively treat this condition. An interesting concept to ameliorate SCI pathology is

to modulate the detrimental neuroinflammation by influencing Mφ polarization. In fact, achieving M2 Mφ excess within the damaged spinal cord is a promising approach to diminish immune-related injury and stimulate tissue repair (58). Various techniques are already suitable which favor M2 Mφ polarization (e.g. direct cytokine administration, gene therapy,…) and, in this way, improve functional recovery after SCI (60). Despite the successes of these techniques, achieving long-lasting M2 Mφ excess and thus enduring repair is not yet obtained. Accordingly, further research still remains necessary to effectively realize and maintain M2 Mφ polarization in case of SCI.

1.5 Interleukin-13

Interleukin- (IL-) 13 is an anti-inflammatory cytokine expressed by various leukocytes, including T helper 2 cells, mast cells and basophils (61-63). This cytokine has an effect on multiple immune cells, including dendritic cells, B-cells, T-cells and Mφs (63). By its distinct anti-inflammatory properties, IL-13 inhibits the expression of pro-inflammatory cytokines and chemokines while stimulating the expression of anti-inflammatory molecules (64). Besides IL-4, IL-13 represents the most important regulator of M2 Mφ polarization. This cytokine stimulates M2 Mφ activation via IL-4/IL-13 mediated signaling pathways. IL-13 signaling is mediated via the interaction of the IL-4 receptor (IL-4R) alpha subunit with the IL-13 receptor alpha 1 subunit. Upon this interaction, IL-13 is able to activate the Janus kinase/signal transducer and activator of transcription (JAK/STAT) signaling and stimulates the transcription of diverse anti-inflammatory genes (e.g. Arginase-1, Ym-1, Fizz). This is mainly mediated via the STAT6 transcription factor (65). Therefore, the therapeutic use of IL-13 is of increasing interest in the case of many inflammatory conditions. In context of SCI, the strong anti-inflammatory properties of IL-13 reduce the pool of pro-inflammatory cells and, as a consequence, create a general anti-inflammatory state. Besides its main anti-inflammatory action, several studies demonstrated neuroprotective and neuroregenerative effects of IL-13 in various neurodegenerative conditions, including multiple sclerosis and Alzheimer's disease (66, 67) .

Due to the therapeutic potential of IL-13, delivery of this cytokine to the neuroinflammatory environment of the spinal cord would be a promising strategy for the treatment of SCI. Several techniques are suitable for the *in vivo* delivery of cytokines. Unfortunately, not all techniques provide sufficient benefit or are ethically appropriate. The most convenient approach would be the intravenous administration of the cytokine of interest. However, this approach can entail serious, sometimes life-threatening, systemic side effects. In case of IL-13, this includes a strong allergic response with respiratory problems and even death as a consequence (68). Another, although heavily criticized, technique to obtain cytokine delivery is gene-therapy. This therapeutic approach involves the use of genes to achieve a temporal or sustained expression of cytokines. Despite being significantly effective, some ethical concerns still withhold a wide dissemination of this technique in modern healthcare. Genetic manipulation *in vivo* is still considered unethical and it is a matter of debate if this technique will be applied in the near future. Therefore, a more alluring possibility to achieve a sustained and efficient *in vivo* delivery of cytokines is via cell-based delivery. This approach comprises the use of cellular material as a vehicle to obtain protein or drug delivery at a desired location within the body. Furthermore, the use of genetically modified cells creates the opportunity to achieve a sustained secretion of the peptide of interest. One of the main advantages

of cell-based delivery is the combination of cell-related characteristics with the delivery of a wide range of peptides (69). Referring to SCI, cell-based delivery of cytokines (e.g. IL-13) is a convenient method to have a sustained impact on the spinal cord's micro-environment. As a result, this approach can modulate the persistent neuroinflammation and influence disease outcome.

As mentioned earlier, IL-13 has both immunomodulatory and reparative properties and hence could improve the neuropathology after SCI. The use of genetically engineered Mφs that secrete IL-13 can be considered to be a promising therapeutic approach to treat SCI, as it combines the immunomodulating properties of IL-13 with the reparative effect of Mφs to inhibit neuroinflammation and improve neurological recovery.

1.6 Project aims

This research project investigates the use of IL-13 secreting Mφs as an approach to improve functional recovery after SCI. During this study, we first investigated whether IL-13 Mφs have anti-inflammatory characteristics and thus can suppress neuroinflammation. These characteristics were evaluated on gene and protein level, both under physiological and inflammatory conditions. Secondly, we determined whether the transplantation of IL-13 Mφs improves functional recovery after SCI in a T-cut hemisection mouse model and whether the underlying mechanism was attributed to IL-13 signaling. For this aim, functional recovery was assessed using the Basso Mouse Scale (BMS) score. Lastly, we investigated the *in vitro* and *in vivo* migration capacity of IL-13 Mφs via a Boyden chamber assay and in a T-cut hemisection mouse model respectively. In this way, this study will shed new light on the potential of genetically engineered Mφs to treat SCI and whether these cells have all the necessary properties to ameliorate this devastating condition.

2 Material and methods

2.1 Animals

All experiments were conducted using 8-12 week old wild type (WT) C57BL/6 mice (Janvier labs, Le Genest-Saint-Isle, France) as well as IL-4R WT and KO BALB/c mice (strain 003514, Jackson Laboratory, Bar Harbor, U.S.). The animals were housed at a conventional animal facility of Hasselt University in a temperature-controlled environment (20°C-25°C) on a 12 hour light-dark schedule and provided with food and water *ad libitum*. Experiments were approved by the local ethical commission of Hasselt University and were conducted according to the guidelines described in the Directive 2010/63/EU on the protection of animals used for scientific purposes.

2.2 T-cut hemisection spinal cord injury

A spinal cord T-cut hemisection was performed as previously described (70). In brief, all mice were anesthetized with 2% isoflurane (Zoetis Belgium S.A., Zaventem, Belgium) and a partial laminectomy was done at thoracic level T8. A T-cut hemisection injury was performed by a complete transection of the left and right dorsal funiculus, the ventral funiculus and the dorsal horns. This model is used to obtain completely transected fibers. After the induced injury, muscles were sutured and the wound was closed using wound clips (BD Autoclip®, BD biosciences, Belgium). Postoperatively, mice received a subcutaneous injection of buprenorphine (0.1 mg/kg body weight, Val d'Hony-Verdifarm nv, Beringen, Belgium) and an intraperitoneal injection of 20% glucose. Eyes were hydrated using NaCl 0.9% (Baxter, Lessines, Belgium). Following these treatments, all mice were placed in a temperature-controlled environment (33°C), until consciousness returned. Bladders were emptied daily, until mice were able to urinate independently.

2.3 Cell transplantation

IL-13 Mφs ($1x10^4$ cells in 2.5 µl) or vehicle (RPMI 1640) were intraspinally injected, 2 mm rostral from the lesion epicenter by using a Hamilton syringe (Hamilton Company, Leuven, Belgium). Transplantation was performed as previously described (71). In brief, mice were placed in a stereotactic frame and cells or vehicle were intraspinally injected with a 32-gauge needle at a rate of 0.625 µl/min for 4 min. After infusion, a saturation time of 4 min was implemented. Finally, the needle was removed and mice were treated as described above.

2.4 Locomotion test

Following SCI, functional recovery was assessed using the BMS score for a period of 28 days. The BMS score is a 10-point rating scale used to assess locomotion based on hind limb movement. The scale ranges from 0 (complete paralysis of the hind limbs) to 9 (normal hind limb movement). Locomotion of all mice were scored in an open field during a 4 min interval. The scoring was done on a daily basis until 7dpi, followed by a scoring every third day until 28dpi. All mice were scored by an investigator blinded to the experimental groups. The mean score of the left and right hind limb was used for the analysis. Mice were excluded when the scores were higher than 1 at 1dpi,

when a sudden drop in score (2 points or more between two consecutive measurements) was observed, or when scores did not increase in 28 days' time.

2.5 Genotyping

Genomic DNA of IL-4R WT and KO BALB/c mice was isolated from tail biopsies after overnight digestion with proteinase K (100µg/ml) in lysis buffer (100mM Tris-HCl, 200mM NaCl, 5mM EDTA, 0.2% SDS) at 55°C. In brief, the digested biopsies were centrifuged at 13,000 rpm for 5 min. Supernatant was collected and ethanol (100%) was added. The samples were mixed, followed by a centrifugation at 13,000 rpm for 10 min. The supernatant was discarded and the pellet was left to dry. Afterwards, the obtained DNA was dissolved in MilliQ. PCR was done using primer pairs to distinguish the *IL4R* WT (5'-TGT GGG CTC AGA GTG ACC AT-3') from the knockout (KO) phenotype (5'-CCA GAC TGC CTT GGG AAA AG-3'; Common: 5'-CAG GGA ACA GCC CAG AAA AG-3'). The KAPA2G Fast HotStart Mouse Genotyping Kit (Sigma-Aldrich, Overijse, Belgium) was used according to manufacturer's instructions. PCR was conducted at 95°C for 2 min, followed by 38 cycles of 95°C for 20 sec, 56.1°C for 15 sec and 72°C for 10 sec, and 72°C for 2 min. PCR products were separated with an 1.5% agarose gel at 120V. DNA fragments were analyzed using Quantity One 1-D Analysis Software (Bio-Rad Laboratories, Temse, Belgium). The size of the obtained DNA fragments are 247 bp for the IL-4R KO mice and 441 bp for the IL-4R WT mice.

2.6 Cell culture

2.6.1 L929 cell culture

NCTC clone 929 (L929) cells were kindly provided by dr. Jeroen Bogie (BIOMED, Diepenbeek, Belgium). L929 cells were cultured in Dulbecco's Modified Eagle's Medium (DMEM, Lonza, Bornem, Belgium), supplemented with 10% heat-inactivated fetal calf serum (hiFCS, Hyclone, Erembodegem, Belgium) and 1% Penicillin/Streptomycin (10.000 U/mL, P/S, Invitrogen, Merelbeke, Belgium). Conditioned medium (CM) of the L929 cells was collected after 10 days and filtered with a 0.2µm filter.

2.6.2 Bone marrow-derived macrophage cell culture

Bone marrow-derived macrophages (BMDMs) were obtained from 8-10 week old female C57BL/6 and BALB/c mice (Janvier Labs). In brief, primary bone marrow cells were isolated from the femur and tibia of these mice by flushing the bone marrow with 1x phosphate buffered saline (PBS). Afterwards, the BMDMs were cultured in RPMI 1640 medium (Lonza) supplemented with 10% hiFCS, 1% P/S, and 15-30% L929 conditioned medium (LCM) for 7 days. Partial or complete medium change was done every 3 days. The BMDMs were seeded in 24-well plates at a density of 150.000 cells/well for *in vitro* experiments. For *in vivo* experiments and transwell migration assays, BMDMs were seeded at the aforementioned density in Corning Costar TC-treated 24 well plates (Sigma-Aldrich). M1 or M2 polarization was obtained by 24h and 48h incubation with 100 ng/ml lipolysaccharide (LPS, PeproTech, Brussels, Belgium) or 33.3 ng/ml recombinant IL-13 (rIL-13, PeproTech), 33.3 ng/mL or recombinant IL-4 (PeproTech) respectively. After polarization, in case of *in vivo* experiments, cells were collected from Corning Costar TC-treated 24 well plates by

rinsing the wells with 1xPBS, or, in case of *in vitro* experiment, lysed for transcript and protein expression analysis. All cells were cultured at 37°C and 5% CO_2.

2.7 Lentiviral transduction

Lentiviral vectors (LV), containing murine IL-13 cDNA, were obtained from the Laboratory for Viral Vector Technology and Gene Therapy (KU Leuven, Leuven, Belgium). For transduction, 150.000 macrophages/well were seeded and cultured in the standardized medium. After cell adhesion, 10µL lentiviral particles were added per well. After 17 hours, the remaining LV particles were removed by medium change. Puromycin selection (2µg/ml, Invitrogen) was performed for 72h. Approximately 50% of the recipient cells were successfully transduced with the IL-13 LV and are termed IL-13 Mφs.

2.8 qPCR

Mice were euthanized by an intraperitoneal injection of sodium pentobarbital (Dolethal, Vetoquinol, France, 200mg/kg), followed by a transcardial perfusion with ringer solution, supplemented with heparin (5.000 IU/mL, Leo Pharma, Lier, Belgium). Both tissue and cell samples were lysed using Qiazol lysis reagent (Qiagen, Hilden, Germany). Total RNA was extracted using the RNeasy mini kit (Qiagen) according to manufacturer's instructions. The amount of isolated RNA was determined via spectrophotometry using a NanoDrop spectrophotometer (Isogen Life Sciences, Utrecht, The Netherlands). cDNA was synthesized using qScript cDNA SuperMix (Quantabio, Beverly, USA). All methods were performed according to manufacturer's instructions. The quantitative polymerase chain reaction (qPCR) was conducted on a StepOnePlus™ detection system (Applied Biosystems, Merelbeke, Belgium) under universal cycling conditions (20 sec at 95°C, 40 cycles of 3 sec at 95°C and 30 sec at 60°C, 15 sec at 95°C, 60 sec at 60°C and 15 sec at 95°C). The mix contained: SYBR™ Green PCR Master Mix (Thermo Fisher Scientific, Merelbeke, Belgium), both 0.3 µM forward and reverse primer of the genes of interest, and cDNA template. Primer details are shown in Table 1, enclosed within the Appendix. Data was processed using StepOne software v2.3. Relative quantification of each transcript was determined using the comparative Ct method. All quantifications were normalized to the expression of the identified housekeeping genes. These genes were identified using the geNorm algorithm. In case of *in vivo* experiments, the identified reference genes were Cyclin A (CycA) and 14-3-3 protein zeta/delta (YWHAZ), while in *in vitro* experiments, CycA, glyceraldehyde 3-phosphate dehydrogenase (GAPDH), and hydroxymethylbilane synthase (HMBS) were identified as the most stable reference genes.

2.9 Western blot

Cell extracts were collected in RIPA lysis buffer supplemented with EASYpack Protease Inhibitor Cocktail (Hoffmann-La Roche, Vilvoorde, Belgium). Protein quantification was done using a Pierce™ BCA Protein Assay Kit (Thermo Fisher Scientific). Samples (4-10 µg) were separated via SDS-PAGE at 200V for 45 min. The Precision Plus Protein™ Dual Color Standards (Bio-Rad Laboratories) was used as a standard. Fractionated proteins were transferred to a polyvinylidene difluoride (PVDF) membrane at 350mA for 1h30 to 2h. The PVDF membranes were blocked with 5% milk (Marvel, Premier foods, Saint Albans, UK) in Tris-buffered saline containing 0.1% Tween 20 (TBS-T) for 1h,

followed by overnight incubation with antibodies against Arg-1 (1:1000, mouse monoclonal, Santa Cruz Biotechnology, Heidelberg, Germany), iNOS (1:500, mouse monoclonal, Sigma-Aldrich), STAT6 (1:1000, rabbit polyclonal, Cell Signaling Technology, Leiden, The Netherlands), p-STAT6 (1:1000, rabbit polyclonal, Cell Signaling Technology) or β-actin (1:2000, mouse monoclonal, Santa Cruz Biotechnology) at 4°C. PVDF membranes were washed with TBS-T and incubated with horseradish peroxidase-conjugated anti-rabbit or anti-mouse antibodies (1:2000, Dako, Leuven, Belgium) diluted in 5% milk TBS-T for 1h at RT. Afterwards, the membranes were washed with TBS-T and proteins were visualized with the Pierce™ ECL Western Blotting Substrate (Thermo Fisher Scientific). Protein expression was quantified using the ImageQuant™ LAS 400 software. All quantifications were normalized to the expression of β-actin, or STAT6 in the case of p-STAT6 quantification.

2.10 ELISA

BMDMs were polarized towards M1 and M2 Mφs as described above. Following polarization, the conditioned medium was collected from the cultured cells. This conditioned medium was also collected from IL-13 Mφs, 72 hours after successful puromycin selection. IL-13 secretion was quantified using the Mouse IL-13 ELISA Ready-SET-Go! kit (Thermo Fisher Scientific), according to manufacturer's instructions.

2.11 Transwell migration assay

Cell culture inserts with a pore size of 8µm (Greiner Bio-One, Vilvoorde, Belgium) were used. BMDMs were suspended in RPMI 1640 medium, supplemented with 1% hiFCS and 1% P/S, and seeded at a density of 200.000 cells per well in the upper compartment of the wells. Cells were incubated at 37°C and 5% CO_2 for 1h in order for the cells to firmly attach to the cell culture inserts. Afterwards, the lower compartment of the wells were filled with RPMI 1640 medium, supplemented with 1% hiFCS, 1% P/S, and various concentrations of stromal cell-derived factor-1 (SDF-1, 0 ng/mL 100 ng/mL, 200 ng/mL, Cell Signaling Technology). Cells were placed back in the incubator in order to migrate from the upper to the lower compartment of the wells. After 16h, the cell culture inserts were removed and cells attached to the upper side of the filter were wiped using cotton swaps. Cells attached to the lower side of the filter were fixed in 4% paraformaldehyde (PFA) for 20 min. After washing with 1xPBS, the cells were stained with 0.1% crystal violet for 45 min. After washing away the abundant staining with 1xPBS, the migrated cells were visualized under a light microscope.

2.12 Immunocytochemistry

Macrophages were seeded on microscope slide coverslips in 24 well plates at a density of 200.000 cells/well. Cells were rinsed in 1xPBS and fixed in 4% PFA for 20 min. After fixation, cells were washed with 1xPBS and permeabilized with 0.05% Triton X-100 in PBS for 30 min at 4°C. After washing three times with 1xPBS, the cells were incubated with 10% protein block (Agilent Technologies, Machelen, Belgium) for 20 min. Cells were rinsed in 1xPBS and incubated with primary antibodies against chitinase 3-like 3 (Ym1, 1:200, rabbit polyclonal, STEMCELL Technologies, Vancouver, Canada) in 10% protein block, overnight at 4°C. Cells were washed with

1xPBS and incubated with Alexa568 secondary antibodies (1:500, goat anti-rabbit, Invitrogen) for 45 min. Negative controls were included by omitting primary antibody incubation and only incubating the selected cells with secondary antibodies. After washing with 1xPBS, cells were counterstained with 4',6-diamidino-2-phenylindole (DAPI) for 10 min. Finally, all coverslips were mounted on microscope glass slides using fluorescent mounting medium (Agilent Technologies, Machelen, Belgium). Images were taken on a Nikon Eclipse 80i microscope (Nikon, Dilbeek, Belgium).

2.13 Immunohistochemistry

Mice were euthanized by an intraperitoneal injection of sodium pentobarbital (Dolethal, Vetoquinol, 200mg/kg), followed by a transcardial perfusion with ringer solution supplemented with heparin (5.000 IU/mL, Leo Pharma) and 4% PFA in 1xPBS. Spinal cords were isolated and submerged in 4% PFA containing 5% sucrose for an overnight post fixation at 4°C, followed by a cryoprotection incubation with 30% sucrose in 1xPBS for 3 days at 4°C. Tissues were embedded in Tissue-Tek O.C.T (Sakura, Alphen aan den Rijn, The Netherlands) and frozen by using liquid nitrogen cooled isopentane. Longitudinal sections of 10µm were obtained using a Leica CM1900 UV cryostat (Leica Biosystems, Diegem, Belgium)

Spinal cord sections were incubated with 10% protein block (Agilent technologies) in 1xPBS for 30 min. Afterwards, the sections were incubated with primary antibodies against myelin basic protein (MBP, 1:250, rat monoclonal, Merck, Darmstadt, Germany) and cluster of differentiation 4 (CD4, 1:250, rat monoclonal, BD Biosciences, Erembodegem, Belgium) in 1% protein block with 0.05% Triton X-100 in 1xPBS, overnight at 4°C. Sections were washed with 1xPBS for 10 minutes and incubated with Alexa fluor 488 secondary antibodies (1:250, goat anti-rat, goat anti-rabbit, Invitrogen) in 1% protein block with 0.05% Triton X-100 in 1xPBS for 1h at RT. Negative controls were included by omitting primary antibody incubation and only incubating the selected sections with secondary antibodies. After washing with 1xPBS, the slides were counterstained with DAPI for 10 min at RT. Afterwards, all sections were mounted with fluorescent mounting medium (Agilent Technologies). Immunohistochemistry pictures were obtained using the Nikon Eclipse 80i microscope (Nikon).

Immunohistochemistry staining for Arg-1 and major histocompatibility complex class II (MHC-II) were performed according to an adapted methodology. Sections were permeabilized by a 30 minute incubation with 0.1% Triton-X100 in TBS. Afterwards, the sections were blocked for 1h with 10% protein block (Agilent Technologies) in TBS. Sections were then incubated with primary antibodies against Arg-1 (1:100, mouse monoclonal, Santa Cruz Biotechnology), and MHC-II (1:200, rat monoclonal, Santa Cruz Biotechnology) in 10% milk-TBS, overnight at 4°C. After rinsing for 5 min with TBS, the slides were incubated with complementary Alexa fluor 488- (1:400, goat anti-rat, Invitrogen) and Alexa fluor 568 (1:400, goat anti-mouse, Invitrogen) secondary antibodies in 10% milk-TBS for 90 min at RT. Negative controls were included by omitting primary antibody incubation and only incubating the selected sections with secondary antibodies. Afterwards, sections were rinsed for 5 min with TBS and then incubated with DAPI for 10 min. After rinsing the slides with TBS and demineralized water, all sections were mounted with fluorescent

mounting medium (Agilent Technologies). Immunohistochemistry pictures were obtained using the Nikon Eclipse 80i microscope (Nikon).

2.14 Statistical analysis

Statistical analysis was performed using Prism 8.01 software (GraphPad Software, San Diego, USA). All data are presented as the mean value ± standard error of the mean (SEM). Normality of the data was assessed using the D'Agostino & Pearson normality test. When data were normally distributed, significance was assessed using a one-way ANOVA with Bonferroni test. BMS scores and percentage of Arg-1^+ cells were analyzed using a two-way ANOVA with a Bonferroni correction for multiple comparisons. If the data were not normally distributed, significance was assessed using a Kruskal-Wallis test with Dunn's multiple comparisons test. Results were considered to be statistically significant when $p<0.05$.

3 Results

3.1 IL-13 Mφs show anti-inflammatory properties and secrete IL-13

The main goal of this research project is to assess whether IL-13 Mφs improve functional recovery after SCI. To do so, IL-13 Mφs should be able to switch the pro-inflammatory environment of the lesion epicenter towards an anti-inflammatory state. Therefore, we first investigated whether IL-13 Mφs have anti-inflammatory properties and, importantly, whether these cells show more potent anti-inflammatory characteristics than *ex vivo* rIL-13 stimulated Mφs. For this aim, the gene, protein and secretion profiles were investigated.

The gene expression of several anti- and pro-inflammatory markers were determined in M0, M1, M2 and IL-13 Mφs via qPCR (figure 2). The selected anti- and pro-inflammatory markers are linked to an M2 (Arg-1, Fizz, CD206 and Ym1) and M1 (iNOS, TNFα, CD38 and CD86) phenotype respectively. As expected, qPCR data showed a significantly increased expression of all anti-inflammatory genes in M2 and IL-13 Mφs compared to M0 Mφs. However, results revealed no significant differences in anti-inflammatory gene expression for Arg-1, Fizz, and CD206 between M2 and IL-13 Mφs (figure 2A). Yet, a trend towards an increased Arg-1 and Fizz expression was present in IL-13 Mφs compared to M2 Mφs. Importantly, a significant difference in Ym1 expression was observed. In case of the pro-inflammatory genes, a significantly increased expression of all genes was observed in M1 Mφs compared to M0 Mφs. Furthermore, expression of all pro-inflammatory genes was significantly decreased in IL-13 Mφs in comparison to M1 Mφs (figure 2B). Furthermore, Arg-1 and iNOS expression were validated on protein level (figure 3). In line with the gene expression data, an upregulation of Arg-1 in IL-13 Mφs was detected compared to M0 Mφs. and a trend towards an increased Arg-1 expression was observed compared to M2 Mφs (figure 3A, B). Furthermore, results showed that iNOS expression was significantly increased in M1 Mφs compared to M0 Mφs. Additionally, the expression of iNOS was significantly decreased in IL-13 Mφs in comparison to M1 Mφs (figure 3C, D). Finally, the secretion of IL-13 was investigated in the conditioned medium (CM) of M0, M1, M2, and IL-13 Mφs by means of an ELISA. Data showed a significantly increased concentration of IL-13 in the CM of IL-13 Mφs compared to M0 and M1 Mφs (figure 3E). No significant difference was observed between M2 and IL-13 Mφs. Additionally, Ym1 expression was investigated in M0, M1, M2 and IL-13 Mφs by means of immunohistochemistry. Results indicated an equal expression between M2 and IL-13 Mφs (Appendix: figure A1).

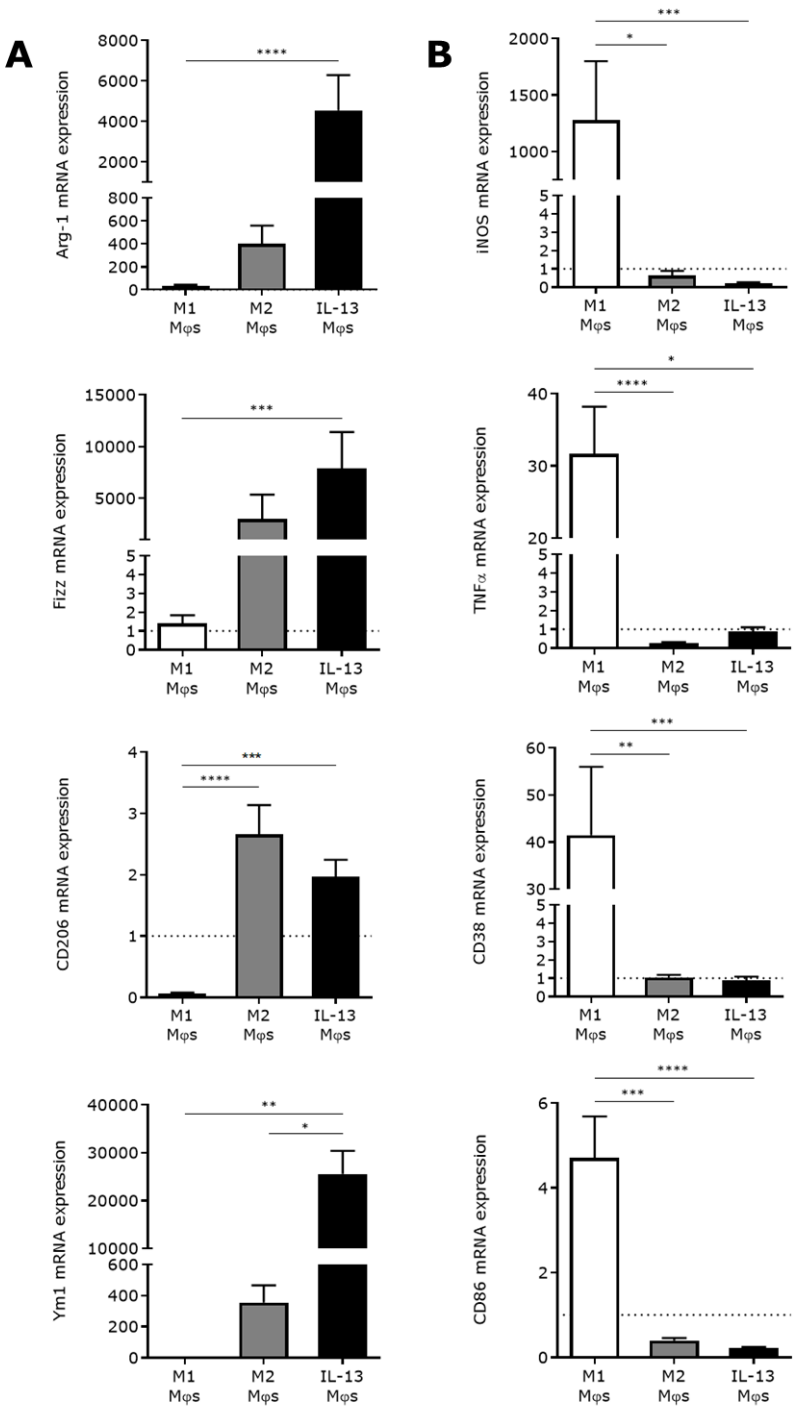

Figure 2: IL-13 Mφs have an M2 phenotype by showing a gene expression profile similar to M2 Mφs. BMDMs were either left unstimulated or were stimulated with 100 ng/mL LPS or 33.3 ng/mL rIL-13 for 24h and 48h respectively to obtain M0, M1 and M2 Mφs. IL-13 Mφs were obtained by transducing BMDMs with lentiviral vectors containing murine IL-13 cDNA. The gene expression of anti- and pro-inflammatory markers were assessed using qPCR. (**A,B**) Expression of commonly used M2 (**A**: Arg-1, Fizz, CD206, and Ym1) and M1 (**B**: iNOS, TNFα, CD38, and CD86) related Mφ markers in M0, M1, M2 and IL-13 Mφs. All data were normalized to the most stable reference genes: CycA, HMBS, and YWHAZ. Fold change was determined compared to M0 Mφs (dotted line). All data are presented as mean ± SEM. n=3-6, Kruskal-Wallis test with Dunn's multiple comparison; *p<0.05, **p<0.01, ***p<0.001, ****p<0.0001. *Arg-1, arginase-1; BMDMs, bone marrow-derived macrophages; CD38, cluster of differentiation 38; CD86, cluster of differentiation 86; CD206, mannose receptor; CycA, Cyclin A; Fizz, resistin like alpha; HMBS, hydroxymethylbilane synthase; IL-13, interleukin-13; iNOS, inducible nitric oxide synthase; LPS, lipopolysacharide; Mφs, macrophages; TNFα, tumor necrosis factor alpha; Ym1, chitinase 3-like 3; YWHAZ, 14-3-3 protein zeta/delta.*

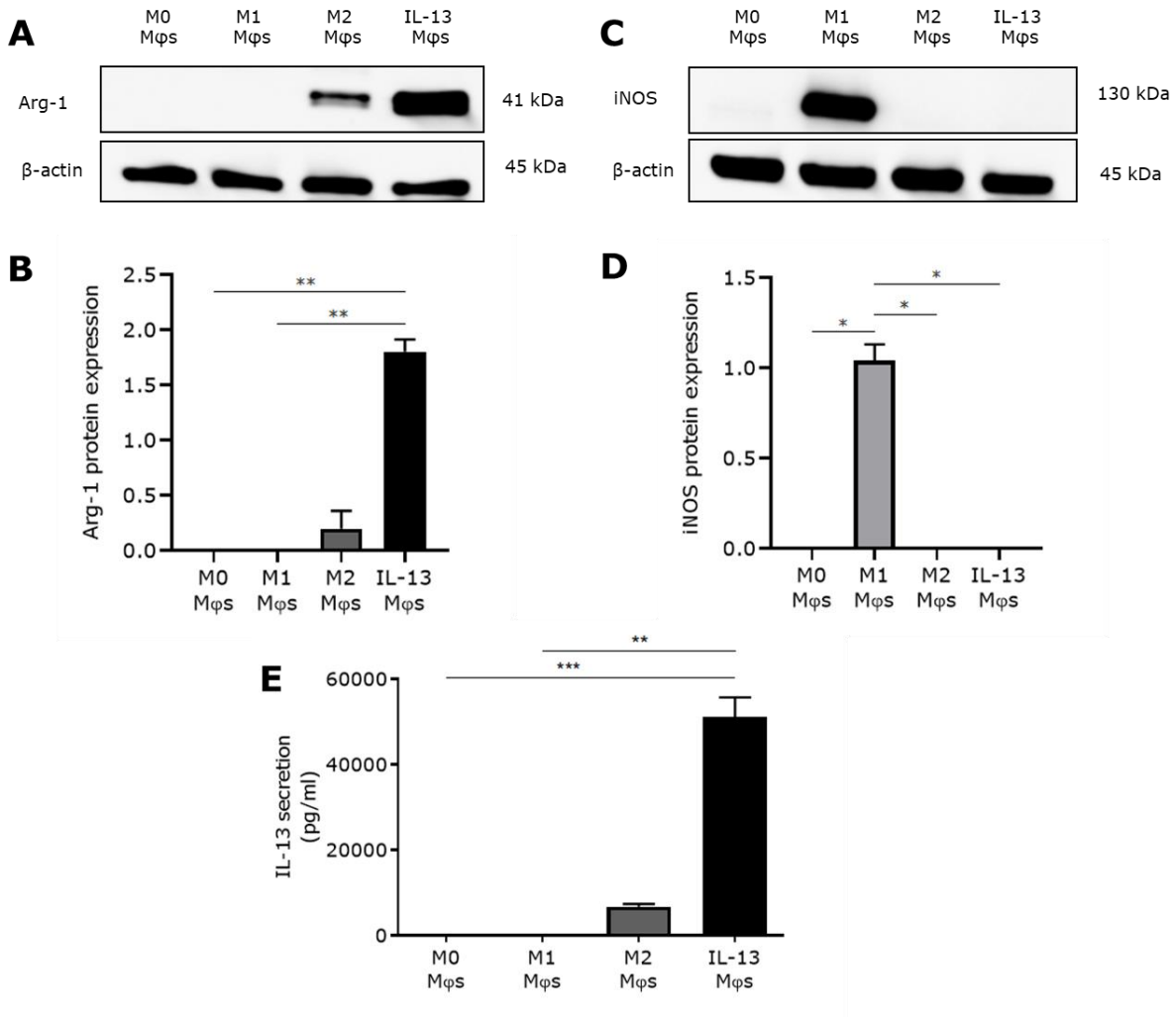

Figure 3: IL-13 Mφs show Arg-1 protein expression and secrete IL-13. BMDMs were either left unstimulated or were stimulated with 100 ng/mL LPS or 33.3 ng/mL rIL-13 for 24h and 48h respectively to obtain M0, M1 and M2 Mφs. IL-13 Mφs were obtained by transducing BMDMs with lentiviral vectors containing murine IL-13 cDNA. (**A-D**) Protein expression of Arg-1 (**A, B**) and iNOS (**C, D**) was assessed using western blot. (**A, C**) Representative western blot images are shown. Data were normalized to β-actin expression. n=3, Kruskal-Wallis test with Dunn's multiple comparison. (**E**) Conditioned medium of M0, M1 and M2 was collected after successful stimulation of the cells. Conditioned medium of IL-13 Mφs was collected after 72h of puromycin selection. The IL-13 concentration in this CM was determined via ELISA. All data are presented as mean ± SEM. n=4, Kruskal-Wallis test with Dunn's multiple comparison, *p<0.05, **p<0.01, ***p<0.001. *Arg-1, arginase-1; BMDMs, bone marrow-derived macrophages; CM, conditioned medium; iNOS, inducible nitric oxide synthase; IL-13, interleukin-13; LPS, lipopolysaccharide; Mφs, macrophages.*

3.2 IL-13 Mφs maintain anti-inflammatory properties under pro-inflammatory conditions

The injured spinal cord is characterized by an excessive pro-inflammatory environment. As this environment drives Mφ polarization towards an M1 phenotype, it is challenging to introduce and maintain anti-inflammatory Mφs within the lesion epicenter. Therefore, we investigated whether IL-13 Mφs are able to maintain their M2 phenotype in the presence of a pro-inflammatory stimulus. For this aim, IL-13 Mφs were either left unstimulated or were exposed to LPS for 24h. Afterwards, the expression of pro- and anti-inflammatory markers was determined by means of qPCR and western blot (figure 4 and 5). Phenotypic properties were compared to those of M2 macrophages to evaluate whether IL-13 Mφs maintain a more potent anti-inflammatory phenotype.

Gene expression of M2 (Arg-1, Fizz, CD206, and Ym1) and M1 (iNOS, TNFα, CD38, and CD86) markers, that were investigated previously, were evaluated (figure 4). qPCR results show significant differences in Arg-1 and Fizz gene expression between LPS-stimulated IL-13 Mφs and LPS-stimulated M0 Mφs (figure 4A). No significant differences were observed in case of CD206 and Ym1 gene expression. Remarkably, no significant differences in the expression of all M2 marker genes were observed between LPS-stimulated IL-13 and M2 Mφs. However, a trend towards an increased expression was present. In case of M1 markers, no significant differences were present between IL-13 and M2 Mφs following LPS stimulation (figure 4B). Nonetheless, there was a trend towards a reduced M1 marker gene expression in LPS-stimulated IL-13 Mφs relative to LPS-stimulated M2 Mφs (figure 5B). Furthermore, Arg-1 and iNOS expression were assessed using western blot (figure 5). Data showed that Arg-1 expression maintained in IL-13 Mφs upon LPS stimulation (figure 5A). However, this phenomenon was also observed in M2 Mφs after LPS stimulation. Moreover, LPS induced iNOS expression in both IL-13 and M2 Mφs (figure 5B).

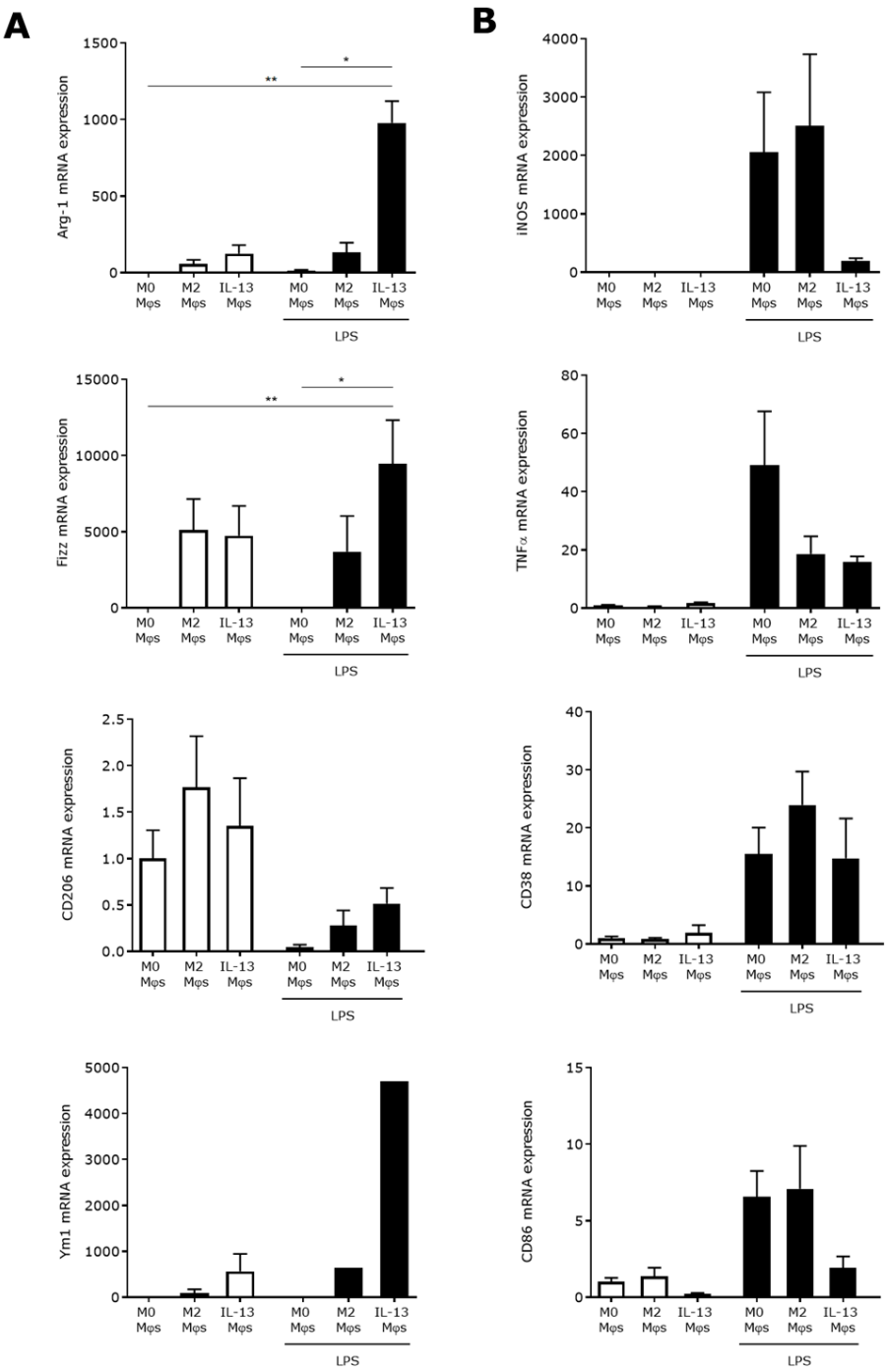

Figure 4: IL-13 Mφs maintain anti-inflammatory gene expression under pro-inflammatory conditions, based on the expression of M2 and M1 Mφ markers. BMDMs were either left unstimulated or were stimulated with 33.3 ng/mL rIL-13 for 48h to obtain M0 and M2 Mφs respectively. IL-13 Mφs were obtained by transducing BMDMs with lentiviral vectors containing murine IL-13 cDNA. Upon macrophage polarization, cells were either left unstimulated or were exposed to 100 ng/mL LPS for 24h. The gene expression of anti- and pro-inflammatory markers was assessed using qPCR. (**A,B**) Expression of commonly used M2 (**A**: Arg-1, Fizz, and Ym1) and M1 (**B**: iNOS, TNFα, CD38, and CD86) related Mφ markers in the concerned cells. All data were normalized to the most stable reference genes: CycA, GAPDH, and HMBS. Fold change was determined compared to M0 Mφs. Data are presented as mean ± SEM. n=4 except for Ym1: n=1, Kruskal-Wallis test with Dunn's multiple comparison, *p<0.05, **p<0.01. *Arg-1, arginase-1; BMDMs, bone marrow-derived macrophages; CD38, cluster of differentiation 38; CD86, cluster of differentiation 86; CD206, mannose receptor; CycA, Cyclin A; Fizz, resistin like alpha; HMBS, hydroxymethylbilane synthase; IL-13, interleukin-13; iNOS, inducible nitric oxide synthase; LPS, lipopolysaccharide; Mφs, macrophages; TNFα, tumor necrosis factor alpha; Ym1, chitinase 3-like 3; YWHAZ, 14-3-3 protein zeta/delta.*

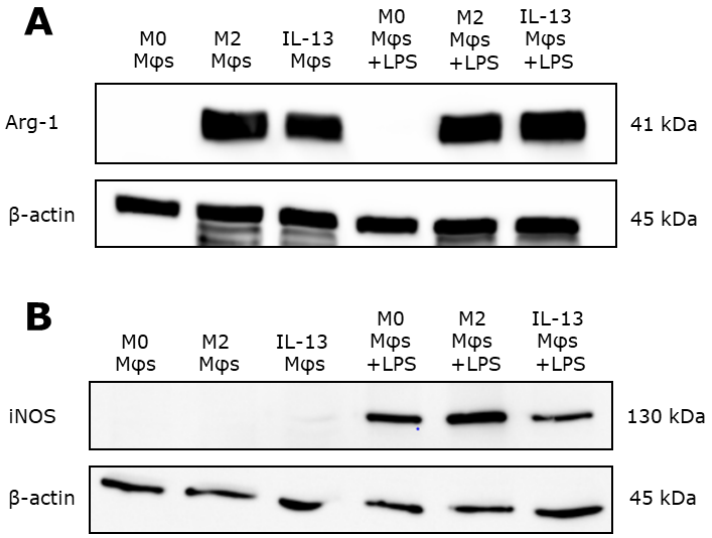

Figure 5: IL-13 Mφs maintain Arg-1 protein expression under pro-inflammatory conditions. BMDMs were either left unstimulated or were stimulated with 33.33 ng/mL rIL-13 for 48h to obtain M0 and M2 Mφs respectively. IL-13 Mφs were obtained by transducing BMDMs with lentiviral vectors containing murine IL-13 cDNA. Upon macrophage polarization, cells were either left unstimulated or were exposed to 100 ng/mL LPS for 24h. (**A-B**) Protein expression of Arg-1 (**A**) and iNOS (**B**) was assessed in the concerned cells using western blot. Representative western blot images are shown. β-actin was used as a loading control. n=1. *Arg-1, arginase-1; BMDMs, bone marrow-derived macrophages; iNOS, inducible nitric oxide synthase; LPS, lipopolysaccharide; IL-13, interleukin-13; Mφs, macrophages.*

3.3 The conditioned medium of IL-13 Mφs induces Arg-1 expression in both M0 and M1 Mφs

Deleterious M1 Mφs are highly present within the injured spinal cord. This M1 excess causes additional damage and limits potential repair. Switching these cells towards an M2 phenotype creates an anti-inflammatory environment, suitable for tissue repair. In order to examine whether IL-13 Mφs are able to suppress neuroinflammation, LPS-stimulated Mφs were treated with the CM of IL-13 Mφs. Subsequently, Arg-1 expression was assessed using western blot (figure 6). Results demonstrated that the CM of IL-13 Mφs was able to induce Arg-1 expression in both M0 and M1 Mφs (figure 6A). However, Arg-1 expression was less defined in M1 Mφs compared to M0 Mφs. Furthermore, data showed that the CM of M2 Mφs was also able to induce Arg-1 expression in M0 Mφs. However, the CM of M2 Mφs did not induce Arg-1 expression in M1 Mφs (figure 6A). Treatment of the Mφs with the CM of M0 and M1 Mφs had no effect on Arg-1 expression.

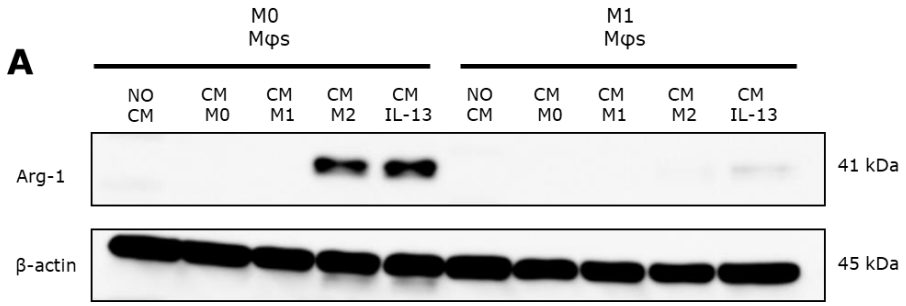

Figure 6: The conditioned medium of IL-13 Mφs stimulates Arg-1 expression in both M0 and M1 Mφs. BMDMs were either left unstimulated or were stimulated with 100 ng/mL LPS for 24h to obtain M0 and M1 Mφs respectively. Afterwards, cells were incubated with the CM of M0, M1, M2 and IL-13 Mφs for 48h. (**A**) Protein expression of Arg-1 was assessed using western blot. Representative western blot image is shown. β-actin was used as a loading control. n=1. *Arg-1, arginase-1; BMDMs, bone marrow-derived macrophages; CM, conditioned medium; LPS, lipopolysaccharide; Mφs, macrophages*

3.4 IL-13 Mφ transplantation improves functional recovery after spinal cord injury in C57BL/6 mice

In vitro experiments revealed the anti-inflammatory properties of IL-13 Mφs. These characteristics are essential to suppress neuroinflammation and improve recovery after SCI. Therefore, IL-13 Mφs have the potential to ameliorate functional outcome *in vivo*. To determine the effect of IL-13 Mφs on functional recovery after SCI, a T-cut hemisection mouse model was used (figure 7A). A trend towards an increased BMS score after IL-13 Mφ transplantation was already observed at 1dpi (figure 7B). A significant difference in BMS score between the IL-13 Mφ- and vehicle-treated mice was observed, beginning at 6dpi and lasting until 28dpi. Furthermore, the differences in BMS score between the IL-13 Mφ- and M2 Mφ-treated mice were also significant, starting at 7dpi until 28dpi. After 28dpi, the difference in BMS score between IL-13 Mφ- and M2 Mφ-treated mice was 1.5 points, while a difference of 2 points was observed between IL-13 Mφ- and vehicle-treated mice. Surprisingly, no difference in BMS score was defined between vehicle- and M2 Mφ-treated mice. Histological analysis showed a significantly increased presence of Arg-1^+ cells at the lesion site of mice treated with IL-13 Mφs compared to M2 Mφ-treated mice (figure 7C). Although, no significant difference in Arg-1^+ cells between M0 Mφ- and IL-13 Mφ-treated mice was observed, a trend towards an increased number in the IL-13 Mφ group was present.

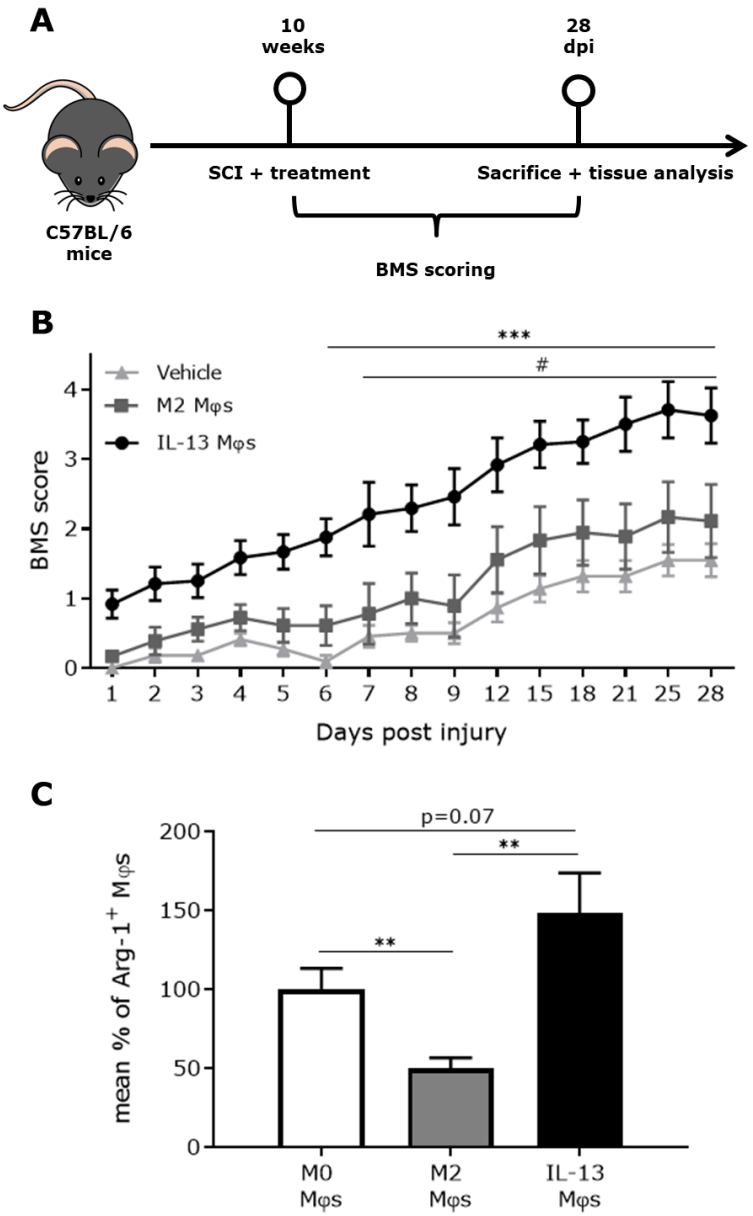

Figure 7: Transplantation of IL-13 Mφs improves functional recovery in C57BL/6 mice after SCI and increases the number of Arg-1$^+$ cells at the lesion site. (**A**) 10-week old C57BL/6 mice were subjected to SCI induction at the eighth thoracic vertebra via a dorsal T-cut hemisection. Immediately following SCI induction, mice received an intraspinal injection with vehicle, M2 or IL-13 Mφs. Functional recovery was evaluated for 28 days after SCI by measuring the BMS score. After this time period, all mice were sacrificed and tissue was histologically analyzed. (**B**) Functional recovery of mice, measured by means of the BMS scoring. $n_{vehicle}$=11, n_{M2}=9, n_{IL-13}=12, Two-way ANOVA with Bonferroni multiple comparison. *, IL-13 Mφs compared to vehicle; #, IL-13 Mφs compared to M2 Mφs. (**C**) Mean number of Arg-1$^+$ Mφs at the lesion site. n_{M0}=6, n_{M2}=4, n_{IL-13}=7, Two-way ANOVA with Bonferroni multiple comparison. Mean number is presented as percentage and normalized to M0 Mφs. All data are presented as mean ± SEM. #p<0.05, **p<0.01, ***p<0.001. *Arg-1, Arginase-1*; *BMS, Basso mouse scale; dpi, days post injury; IL-13, interleukin-13; Mφs, macrophages; SCI, spinal cord injury.*

3.5 Transplantation of IL-13 Mφs improves functional recovery after SCI via IL-13 signaling

After observing a positive effect of IL-13 Mφ transplantation on functional recovery after SCI, we investigated the underlying mechanism. The improvement in locomotor function due to IL-13 Mφ transplantation is either caused by IL-13 signaling or the introduction of anti-inflammatory Mφs within the neuroinflammatory environment of the lesion. To determine which event is responsible for the observed effect, transgenic mice with a disrupted IL-13 signaling were used. Therefore, IL-4R wild type (WT) and knockout (KO) BALB/c mice were selected, as the IL-4R is essential in IL-13 signaling. Genotyping of the mice confirmed KO of the IL-4R gene (Appendix: figure A2). SCI was induced in all mice, after which they were treated with either a vehicle or IL-13 Mφs. Prior to the described *in vivo* experiment, disrupted IL-4R signaling was evaluated. Mφs of both IL-4R WT and KO BALB/c mice were isolated. It was determined whether these cells were able to polarize towards M2 Mφs upon IL-4 and IL-13 stimulation (figure 8). Protein expression of Arg-1 was assessed in IL-4R WT and KO BMDMs, either left unstimulated or stimulated with IL-4 or IL-13 (figure 8A-D). Results revealed that IL-4 and IL-13 stimulation of IL-4R WT Mφs induced Arg-1 expression. Furthermore, it was observed that neither upon IL-4 nor IL-13 stimulation induced Arg-1 expression in IL-4R KO cells. Moreover, disrupted IL-4R signaling was further validated by assessing p-STAT6 and STAT6 protein expression in the concerned cells. As STAT6 becomes phosphorylated upon IL-4R stimulation, KO of the specified receptor prevents this phosphorylation and thus, downstream signaling of IL-4 and IL-13. Western blot analysis revealed a lack of p-STAT6 expression in IL-4R KO Mφs upon IL-4 and IL-13 stimulation (figure 8E, F). p-STAT6 expression was only present in IL-4R WT Mφs stimulated with either IL-4 or IL-13. Data showed that STAT6 expression was present in all cells. Following *in vitro* confirmation of the disrupted IL-4R signaling, the underlying mechanism regarding functional improvement was investigated. It was assessed whether IL-13 Mφs exerted their positive effect via IL-13 signaling (figure 9). Functional recovery was assessed for 28 days after SCI in IL-4R WT and KO mice, subjected to an intraspinal vehicle injection or IL-13 Mφ transplantation (figure 9A). A significant difference in BMS score was observed between IL-13 Mφ-treated IL-4R WT mice and all other conditions at 9dpi and lasting until 28dpi (figure 10B). BMS scores of IL-13 Mφ-treated IL-4R KO mice were similar to vehicle-treated mice. Immunohistochemical analysis revealed that there was no significant difference in demyelinated area nor in T-cell numbers within the lesion site between all conditions (figure 10C).

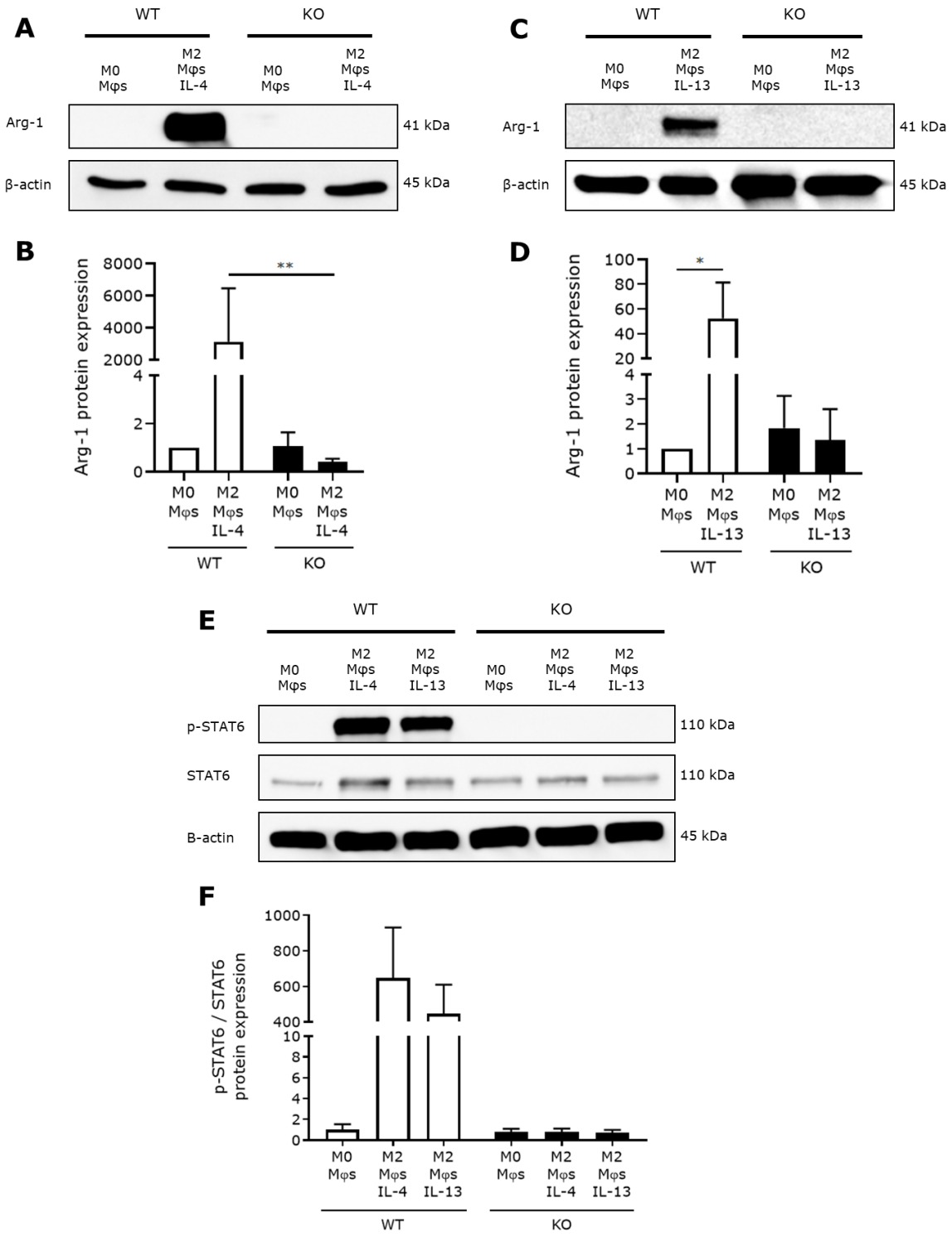

Figure 8: M2 Mφ polarization is absent in Mφs obtained from IL-4R KO BALB/c mice, confirming disrupted IL-4R signaling. BMDMs were obtained from IL-4R WT and KO BABLB/c mice and were either left unstimulated or were stimulated with 33 ng/mL IL-4 or IL-13 for 48h to achieve M0 and M2 Mφ polarization respectively. Protein expression of Arg-1 (**A-D**) and p-STAT6/STAT6 (**E-F**) was determined in IL-4R WT and KO Mφs, stimulated with IL-4 or IL-13 by using western blot. Data were normalized to β-actin (in case of Arg-1) or STAT6 (in case of p-STAT6) expression and further normalized to WT M0 Mφs. All data are presented as mean ± SEM. $n_{Arg\text{-}1}$=4, $n_{p\text{-}STAT6/STAT6}$=3, Kruskal-Wallis test with Dunn's multiple comparison, *p<0.05, **p<0.01. *Arg-1, Arginase-1; BMDMs, bone marrow-derived macrophages; IL-4, interleukin-4; IL-13, interleukin-13; IL-4R, interleukin-4 receptor; KO, knockout; Mφs, macrophages; p-STAT6, phosphorylated-signal transducer and activator of transcription 6; STAT6, signal transducer and activator of transcription 6; WT, wild type.*

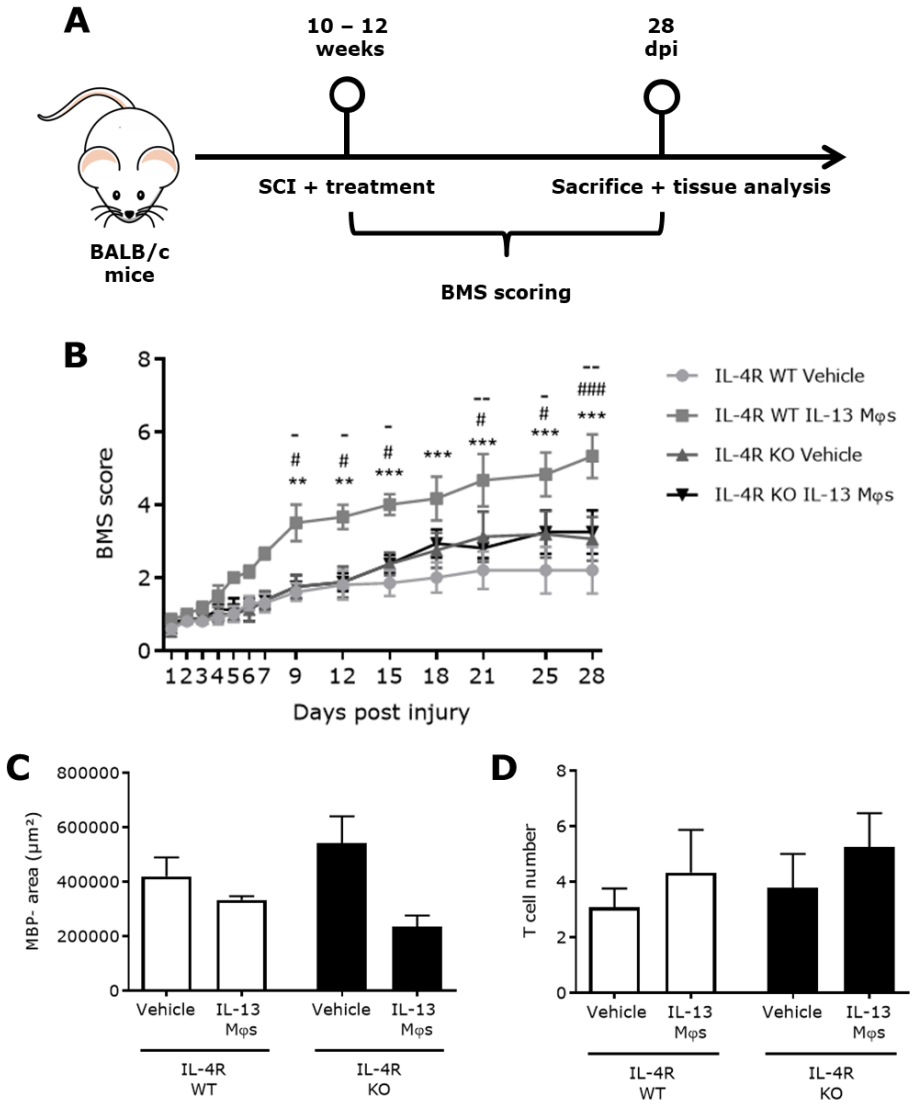

Figure 9: Transplantation of IL-13 Mφs improves functional recovery after SCI in WT but not in IL-4R KO BALB/c mice. (**A**) 10- to 12-week old IL-4R WT and KO BALB/c mice were subjected to SCI induction at the eighth thoracic vertebra via a dorsal T-cut hemisection. Immediately following SCI induction, all mice received an intraspinal injection either with vehicle or IL-13 Mφs. Functional recovery was evaluated for 28 days after SCI by measuring the BMS score. After this time period, all mice were sacrificed and spinal cord tissue was analyzed. (**B**) Functional recovery of IL-4R WT and KO mice, measured by means of the BMS scoring. $n_{vehicle,\ WT}$=5, $n_{IL\text{-}13,\ WT}$=3, $n_{vehicle,\ KO}$=4, $n_{IL\text{-}13,\ KO}$=4, Two-way ANOVA with Tukey's multiple comparison. *, IL-4R WT vehicle compared to IL-4R WT IL-13 Mφs; #, IL-4R WT IL-13 Mφs compared to IL-4R KO vehicle; -, IL-4R WT IL-13 Mφs compared to IL-4R KO IL-13 Mφs. (**C, D**) The demyelinated area (**C**) and T-cell number (**D**) in spinal cord tissue of the concerned mice. $n_{vehicle,\ WT}$=4, $n_{IL\text{-}13,\ WT}$=3, $n_{vehicle,\ KO}$=4, $n_{IL\text{-}13,\ KO}$=3, Kruskal-Wallis test with Dunn's multiple comparison. All data are presented as mean ± SEM. $^{\#/-}p<0.05$, $^{**/--}p<0.01$, $^{***/\#\#\#}p<0.001$. *BMDMs, bone marrow-derived macrophages; BMS, Basso mouse scale; dpi, days post injury; IL-4, interleukin-4; IL-13, interleukin-13; IL-4R, interleukin-4 receptor; KO, knockout; Mφs, macrophages; MBP, myelin basic protein; SCI, spinal cord injury; WT, wild type.*

3.6 Optimization of Boyden chamber assay in order to investigate macrophage migration *in vitro*

To determine whether IL-13 Mφs migrate towards sites of neuroinflammation, we investigated the migratory capacity of these cells in case of SCI. Various chemokines are involved in the attraction of Mφs towards the injured spinal cord. SDF-1 is one of those chemokines and is considered the most potent chemoattractant of Mφs in case of SCI. To analyze the ability of IL-13 Mφs to migrate towards various concentrations of SDF-1, a Boyden chamber assay was performed. The migration of M0, M1, M2 and IL-13 Mφs towards different concentrations of SDF-1 (0 ng/mL, 100 ng/mL, and 200 ng/mL) was investigated. Visualization of the migrated cells showed no differences in cell migration between all cell types (figure 10). In addition, the various concentrations of SDF-1 had no effect on cell migration. This indicates that neither the concentration of SDF-1 nor the cell type showed was a crucial factor in the migration of Mφs.

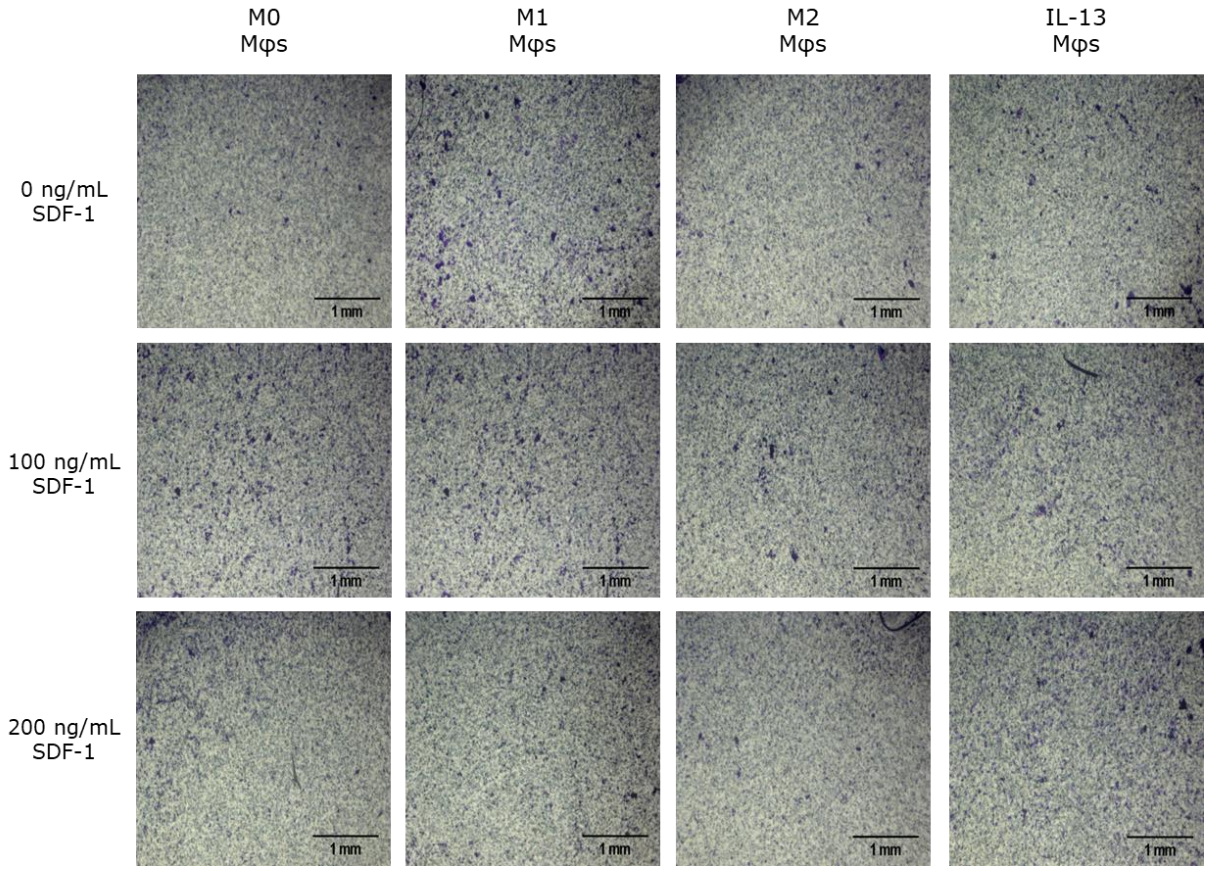

Figure 10: IL-13 Mφs do not migrate towards several concentrations of SDF-1. BMDMs were either left unstimulated or were stimulated with 100 ng/mL LPS or 33.3 ng/mL rIL-13 for 24h and 48h respectively to obtain M0, M1 and M2 Mφs. IL-13 Mφs were obtained by transducing BMDMs with lentiviral vectors containing murine IL-13 cDNA. All cells were exposed to 0 ng/mL, 100 ng/mL or 200 ng/mL SDF-1 and migration after 16h, through a cell culture insert (pore size of 8µm), was evaluated. Migrated cells were stained with crystal violet and visualized. n=1. *BMDMs, bone marrow-derived macrophages; IL-13, interleukin-13; LPS, lipopolysaccharide; Mφs, macrophages*; *SDF-1, stromal cell-derived factor-1.*

3.7 IL-13 Mφs are not able to migrate towards the lesion epicenter and alter the inflammatory environment of the spinal cord at 7 days post injury

Previous experiments showed that Arg-1^+ cells were highly present at the lesion site of the injured spinal cord after IL-13 Mφ transplantation. As IL-13 Mφs are characterized by Arg-1 expression, this finding indicates the possibility of IL-13 Mφs to migrate towards the lesion epicenter and locally exert positive effects. Therefore, migration of IL-13 Mφs was evaluated in mice by assessing the gene expression of lentiviral-derived IL-13 (LV IL-13), as this gene is solely originating from the LV-transduced IL-13 Mφs. Migration was assessed at 0 and 7dpi by determining the presence of IL-13 Mφs at the site of injection and the lesion site (figure 11). Prior to qPCR analysis, primer efficiency of the LV IL-13 gene primers were evaluated. qPCR revealed that the selected primers were able to detect the expression of LV-13 in IL-13 Mφs, in contrast to M0, M1 and M2 Mφs which showed no expression (figure 11A). Furthermore, qPCR results showed that LV IL-13 expression was present at the injection site of IL-13 Mφ treated mice at 0dpi. Surprisingly, at 7dpi, neither at the injection nor at the lesion site, LV-IL-13 expression was observed in IL-13 Mφ treated mice (figure 10B). Additionally, to investigate the effect of IL-13 Mφs on the inflammatory state of the spinal cord, expression of M2 (Arg-1, Ym1) and M1 (iNOS, MHC-II) markers at the injection and lesion site was determined. Results showed that the expression of Arg-1 was reduced at the lesion site of IL-13 Mφ treated mice compared to vehicle treated mice at 7dpi (figure 10C, D). However, no significant differences were observed. Likewise, no differences in Ym1 expression was present between IL-13 Mφ- and vehicle-treated mice. The expression of iNOS and MHC-II were reduced at the lesion site of IL-13 Mφ treated mice compared to vehicle treated mice at 7dpi (figure 14B). Again, no significant differences were observed.

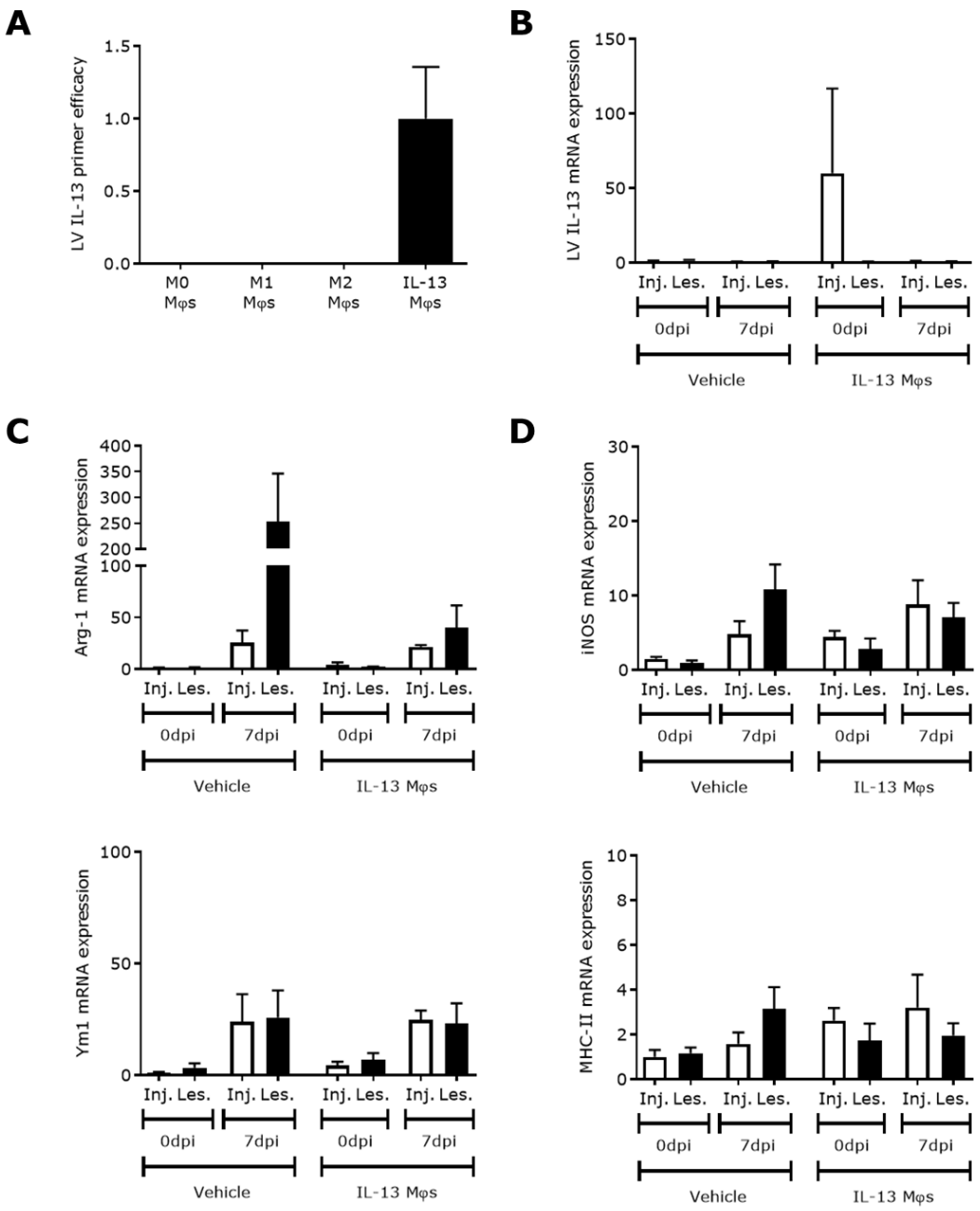

Figure 11: IL-13 Mφs do not migrate towards the lesion epicenter and do not alter the inflammatory environment of the spinal cord within 7dpi. (**A**) BMDMs were either left unstimulated or were stimulated with 100 ng/mL LPS or 33.3 ng/mL rIL-13 for 24h and 48h respectively to obtain M0, M1 and M2 Mφs. IL-13 Mφs were obtained by transducing BMDMs with lentiviral vectors containing murine IL-13 cDNA. LV IL-13 gene expression was assessed in M0, M1, M2 and IL-13 Mφs by use of specific primers. Primer efficacy is presented as relative LV IL-13 mRNA expression. Data were normalized to the expression of the most stable reference genes: CycA, GAPDH, and HMBS, and further normalized to IL-13 Mφs. n=5, Kruskal-Wallis test with Dunn's multiple comparison. (**B**) LV IL-13 gene expression was assessed at 0 and 7dpi, at the injection and lesion site of mice treated with either a vehicle or IL-13 Mφs. (**C**,**D**) M2 (Arg-1, Ym1) (**C**) and M1 (iNOS, MHC-II) (**D**) gene expression was assessed at 0 and 7dpi, at the injection and lesion site of mice treated with either a vehicle or IL-13 Mφs. All data were normalized to the most stable reference genes: CycA, and YWHAZ and further normalized to the expression at the injection site of vehicle-treated mice at 0dpi. All data are presented as mean ± SEM. $n_{vehicle,\ 0dpi}=3$, $n_{vehicle,\ 7dpi}=6$, $n_{IL\text{-}13,\ 0dpi}=4$, $n_{IL\text{-}13,\ 7dpi}=6$, Kruskal-Wallis with Dunn's multiple comparison. *Arg-1, arginase-1;* CycA, Cyclin A; *dpi, days post injury; GAPDH, glyceraldehyde 3-phosphate dehydrogenase; HMBS, hydroxymethylbilane synthase; Inj., injection site; iNOS, inducible nitric oxide synthase; Les, lesion site; MHC-II, major histocompatibility complex class II; Mφs, macrophages; Ym1, chitinase 3-like 3.*

4 Discussion

Mφs are key players in the inflammatory response following spinal cord injury, either causing extensive damage or inducing tissue repair (50). Many studies observed that an M2 Mφ excess within the injured spinal cord resulted in an improved functional outcome and neural repair (55, 72). Mφ polarization is therefore an important aspect of SCI outcome and can be influenced by various local cytokines and other factors. In this context, several studies demonstrated the neuroprotective and neuroregenerative properties of IL-13 (66, 73, 74). Therefore, we hypothesized that the use of genetically modified Mφs, which secrete IL-13, improve functional outcome after SCI by locally exerting M2 effects and secreting IL-13.

Firstly, we investigated whether IL-13 Mφs indeed have anti-inflammatory characteristics and whether these are more potent than those observed in M2 Mφs. Therefore, the gene and protein expression of anti- and pro-inflammatory markers were assessed. Gene expression of anti-inflammatory markers only showed significant difference between both cell types in Ym1 expression (figure 2A). Nevertheless, a trend towards increased Arg-1 and Fizz expression in IL-13 Mφs compared to M2 Mφs was present. Furthermore, Arg-1 protein levels showed a trend towards increased Arg-1 expression in IL-13 Mφs (figure 3A, B). These increased trends, both on gene and protein level, indicate that there might be an upregulation of anti-inflammatory markers in IL-13 Mφs compared to M2 Mφs. However, due to the low sample size, significant differences were absent. The increased trends of anti-inflammatory marker expression in IL-13 Mφs was attributed to autocrine polarization of the cells. We demonstrated IL-13 secretion in the CM of IL-13 Mφs (figure 3E). IL-13 binds to the IL-13R, located on the Mφs and consequently stimulates M2 related transcription. In line with our results, several studies illustrate that IL-13 induces M2 polarization and stimulates the upregulation of anti-inflammatory mediators of which the most important one is Arg-1 (75, 76). Due to the sustained secretion of IL-13 by the IL-13 Mφs, a persistent activation of the IL-13R is present and thus, expression of anti-inflammatory markers is continuously stimulated. Importantly, differences in pro-inflammatory gene expression were not observed between IL-13 and M0 Mφs (figure 2B). These findings are beneficial, because a study of *Boehler et al.* showed an upregulation of TNFα in macrophages transduced with LV vectors (77). In fact, LV transduction can elicit a pro-inflammatory response in macrophages, thereby upregulating the expression of pro-inflammatory markers. However, secretion of IL-13 was able to counteract the pro-inflammatory response following LV transduction, further confirming the potent anti-inflammatory effect of IL-13. Based on the obtained data, IL-13 Mφs show anti-inflammatory properties comparable to M2 Mφs. However, the use of IL-13 Mφs in case of SCI is more convenient than the use of M2 Mφs due to the secretion of IL-13. In this way, not only autocrine stimulation is obtained but also paracrine macrophage polarization is attainable. This makes sure that both IL-13 Mφs, as well as surrounding Mφs have an M2 phenotype. In contrast, M2 Mφs do not have the ability to secrete IL-13, thereby lacking a potent autocrine stimulation and making these Mφs more dependable of cytokines from their environment. In case of SCI, mainly pro-inflammatory cytokines are present within the injured spinal cord, making M2 Mφs more prone to switch towards an M1 phenotype. Therefore, the use of IL-13 Mφs as an alternative to M2 Mφs is a more convenient and more effective approach in the treatment of SCI.

The lesion epicenter is characterized by a distinct pro-inflammatory environment. In order to stimulate functional repair, IL-13 Mφs must be able to survive the detrimental pro-inflammatory stimuli and maintain their anti-inflammatory properties. We investigated whether IL-13 Mφs maintained the expression of anti-inflammatory markers under pro-inflammatory conditions and if this was different from M2 Mφs. To assess the phenotypic characteristics of IL-13 Mφs in a pro-inflammatory environment, the gene and protein expression of anti- and pro-inflammatory markers were assessed in IL-13 Mφs exposed to LPS and compared to those in M2 Mφs. Data showed that there was a trend towards increased expression of the anti-inflammatory markers Arg-1, Fizz, and Ym1 in LPS-stimulated IL-13 Mφs compared to LPS-stimulated M2 Mφs (figure 4A). However, due to the low sample size, a significant difference was not observed. The increased expression of anti-inflammatory markers in LPS-stimulated IL-13 Mφs indicates that these cells show anti-inflammatory properties, even under pro-inflammatory conditions. Likewise, a trend towards a decrease of pro-inflammatory gene expression was present in LPS-stimulated IL-13 Mφs compared to M2 Mφs (figure 4B). This finding indicates a difference between IL-13 and M2 Mφs in maintaining their phenotype under pro-inflammatory conditions. However, no significant difference was observed. The observed trend indicates that M2 Mφs are possibly more prone to an M1 switch compared to IL-13 Mφs. This phenomenon can be explained by the continuous stimulation of IL-13 Mφs by the secretion of IL-13. This is in contrast to the selected M2 Mφs which only had a single stimulation of IL-13. The more potent effect of a continuous stimulation compared to a single stimulation has been shown before. *Boehler et al.* demonstrated that the continuous secretion of IL-10 by transduced Mφs enhanced the anti-inflammatory properties of these cells compared to a single stimulation of IL-10. Therefore, upon interferon-γ stimulation, a less distinct M1 switch was observed in the transduced Mφs (77). Due to the secretion of IL-13 and thus, the continuous stimulation of the IL-13 Mφs, these cells are less responsive to pro-inflammatory stimuli and less prone to an M1 switch. However, we observed that the expression of all pro-inflammatory markers increased in both M2 and IL-13 Mφs upon LPS stimulation. However, the increase in pro-inflammatory gene expression in IL-13 Mφs was less distinct compared to M2 Mφs, validating the counteracting effect of IL-13 secretion. Contradictory, we also observed that the expression of Arg-1, Fizz, and Ym1 increased upon LPS stimulation. These results are in line with the findings of Fenn *et. al* who showed that Arg-1 expression significantly increased after IL-4R activation upon LPS stimulation (78). They showed that LPS-activated microglia/macrophages are more prone to IL-4R stimulation compared to unstimulated microglia/macrophages. As mentioned before, IL-13 binds to a subunit of the IL-13R, followed by its dimerization with a subunit of the IL-4R. This results in activation of the latter and downstream signaling pathways. The activation of the IL-4R by IL-13 explains the increase in anti-inflammatory gene expression in IL-13 Mφs upon LPS stimulation. The gene expression results were validated on protein level. Arg-1 and iNOS expression were assessed in IL-13 Mφs after LPS stimulation. However, no differences were observed in expression of both proteins between LPS-stimulated IL-13 and M2 Mφs (figure 5A, B). However, as this experiment was only conducted once, conclusions cannot be made yet. To summarize, gene expression analysis of the IL-13 Mφs shows that these cells have anti-inflammatory properties, even under pro-inflammatory conditions. However, differences between M2 Mφs have yet to be investigated.

Previously, we confirmed the anti-inflammatory characteristics of IL-13 Mφs under pro-inflammatory conditions. However, to be able to improve functional recovery after SCI, IL-13 Mφs should not merely exert M2 functions. These cells should also switch the pro-inflammatory environment of the lesion epicenter towards an anti-inflammatory state, thereby suppressing neuroinflammation, stimulating neural repair and thus improve functional outcome. This important feature was investigated *in vitro*. We determined whether IL-13 Mφs, and more specifically the IL-13 secretion of these cells, stimulates M1 Mφs to polarize towards an M2 phenotype. Therefore, Arg-1 protein expression of M1 Mφs, stimulated with the CM of IL-13 Mφs, was determined. Western blot analysis revealed that Arg-1 expression was observed in M1 Mφs stimulated with the CM of IL-13 Mφs (figure 6A). Additionally, stimulating M0 Mφs with the CM of IL-13 Mφs also induces Arg-1 expression in the concerned cells, but no difference was observed between M2 and IL-13 Mφs CM stimulation. Due to the low sample size (n=1) of this experiment, no definitive conclusions can be drawn. However, the observation of Arg-1 expression in M1 Mφs, stimulated with the CM of IL-13 Mφs, indicates that IL-13 Mφs are able to switch Mφs towards an M2 phenotype. This is in line with multiple studies which observed that M1 Mφs show anti-inflammatory properties following IL-13 stimulation (79, 80). For instance, *Sinha et al.* demonstrated that IL-13 stimulation of M1 Mφs resulted in a lower nitric oxide production compared to M1 Mφs. Within this study, an IL-13 concentration of 50 ng/mL was used. This concentration is equal to the one we observed in the CM of IL-13 Mφs. This finding suggests that the CM of IL-13 Mφs will be able to stimulate M1 Mφs to show anti-inflammatory properties. However, additional experiments are required to validate this theory.

Previous results within this research showed that IL-13 Mφs have an anti-inflammatory phenotype, even in a pro-inflammatory environment, and that these cells possibly have the ability to induce an M2 phenotype switch in M1 Mφs. All these properties are favorable and essential in the recovery of SCI, as it suppresses neuroinflammation and induces neural repair. Therefore, we considered that the use of IL-13 Mφs would be an ideal approach to improve functional outcome after SCI. Accordingly, we investigated whether transplantation of IL-13 Mφs improves functional recovery in a T-cut hemisection mouse model. Data illustrated that IL-13 Mφ transplantation significantly improved functional recovery after SCI (figure 7B). A trend towards an increased BMS score was already observed in IL-13 Mφ treated mice compared to vehicle treated mice at 1 dpi. This could be explained by a potential neuroprotective effect of IL-13. Multiple studies already indicated the neuroprotective effects of IL-13 in neurological disorders, including SCI (66, 74, 81). As secondary injury occurs within minutes after SCI, neuroprotective agents exert their effect by protecting neurons and oligodendrocytes. In case of SCI, this neuroprotective effect can result in a reduced extent of neural damage and functional disability. However, this theory requires further investigation but opens up an interesting aspect of the IL-13 Mφs. After a period of 28 days, mice which received IL-13 Mφ transplantation showed an improvement in recovery of 2.0 points in BMS score compared to vehicle-treated mice. Mice which received a vehicle were not able to properly place their hind limbs during locomotion, while IL-13 Mφ transplantation resulted in proper paw placement and weight support on both limbs. These findings are consistent with earlier obtained results within our research group which showed that mesenchymal stem cell (MSC)-based delivery of IL-13 resulted in an improved functional and histopathological outcome after SCI (71). These

findings indicate the importance of IL-13 in functional recovery. However, differences between Mφs and MSCs have been observed as well. These differences could be explained by the effect of MSCs on macrophages after SCI. Several studies indicate that MSCs improve functional recovery after SCI by promoting M2 activation (82-84). This finding illustrates that MSCs have a paracrine effect on resident immune cells and by these means suppress neuroinflammation. However, IL-13 Mφs show both paracrine and autocrine effects. The enhanced effect of Mφs is evident on the level of functional outcome. The use of Mφs was able to further improve the beneficial effect of IL-13 compared to MSCs. For instance, the use of genetically engineered macrophages resulted in an improvement of 2.1 points in BMS score compared to a vehicle, while the use of genetically engineered MSCs led to an improvement of 1.1 points in BMS score compared to a control (71). Therefore, the use of IL-13 Mφs is possibly a better therapeutic approach in treating SCI compared to MSCs. However, further experiments still remain necessary to investigate the difference between Mφs and MSCs on functional and histopathological recovery after SCI. Histological analysis indicated that the number of Arg-1^+ Mφs in the lesion site of IL-13 Mφ treated mice significantly increased (figure 7C). The pool of Arg-1^+ Mφs possibly consists of anti-inflammatory Mφs, stimulated by IL-13 derived from the IL-13 Mφs. This phenomenon was also observed by *Dooley et al.* who showed that IL-13 secreting MSCs increased the number of Arg-1^+ Mφs in the lesion epicenter of the injured spinal cord (71). However, another possible explanation for the increase in Arg-1^+ Mφs is the presence of IL-13 Mφs. As these cells are characterized by Arg-1 expression, IL-13 Mφs possibly migrate towards the lesion epicenter and thus, locally exert their effects. This migratory ability is in contrast to the findings in MSCs, as these cells do not have the ability to migrate towards the lesion epicenter, further strengthening the benefits of IL-13 Mφs over MSCs (85).

In order to assess whether the observed improvement in functional outcome was attributed to IL-13 signaling, we investigated the effect of IL-13 signaling on functional recovery. Induction of IL-13 signaling is mediated via the binding of IL-13 to a subunit of the IL-13R (i.e. the IL-13Rα1 subunit). Next, this subunit forms a dimer with the IL-4Rα subunit of the IL-4R. This dimerization results in the activation of the formed receptor and subsequently, downstream transduction of the concerned signal. As IL-13 signaling is dependent on the IL-4R, we aimed to block this signaling cascade via KO of this receptor. Therefore, an IL-4R KO mouse model was used. BMS scores of both IL-4R WT and KO mice revealed that functional improvement was only observed in IL-4R WT mice (figure 9B). This finding indicates that benefits in functional outcome after IL-13 Mφ transplantation are contributed to IL-13 signaling. As IL-13 is one of the most potent M2 macrophage polarization factors, it has the ability to suppress pro-inflammatory signaling, thereby creating an anti-inflammatory environment (86, 87). Furthermore, various studies revealed that IL-13 stimulates neural growth and is involved in both protection and repair of CNS structures (66, 74, 88). Therefore, functional improvement after IL-13 Mφ transplantation is due to the activated IL-13 signaling, which results in immunomodulation, neuroprotection and neural repair. Nonetheless, the neuro-protective and –regenerative properties of IL-13 Mφs still require further investigation. An important issue to mention is that the IL-4R KO model not only shows disrupted IL-13 signaling. IL-4 is another anti-inflammatory cytokine which exerts its effects by binding and activating the IL-4R. Therefore, disrupted IL-4 signaling can be partly responsible for the absence

of functional improvement in the IL-4R KO mice. This makes the IL-4R KO model not the ideal model to solely investigate the effect of IL-13 signaling on functional recovery. For this particular reason, it is recommended to repeat the indicated experiment in an IL-13R KO model. As IL-13 signaling requires the binding of IL-13 to both an IL-4R and IL-13R subunit, the IL-13R KO model should only have an IL-13R subunit KO. However, within this research, the impeded IL-4 signaling had no impact on the functional recovery of IL-4R KO mice compared to wild type mice. To investigate whether IL-4 is an important cytokine in the response to SCI, its expression can be assessed both on gene and protein level within the injured spinal cord. If no change in IL-4 expression is observed after IL-4R KO, the only differences in functional recovery can be attributed to the effect of IL-13.

Within this research, a difference in functional recovery between C57BL/6 and BALB/c mice was observed. After IL-13 Mφ transplantation, BALB/c mice showed a more pronounced functional improvement compared to C57BL/6 mice (3.1 points in BALB/c mice vs. 2.1 points in C57BL/6 mice). This has been observed before and can be ascribed to the phenomenon that BALB/c mice are more T helper 2 adjusted while C57BL/6 mice are more T helper 1 adjusted (89, 90). This more pronounced anti-inflammatory orientation in the BALB/c mice is beneficial in case of SCI outcome and can be a possible explanation for the observed difference in functional recovery between both mouse strains. Histological analysis revealed that IL-13 Mφ transplantation did not have an effect on T-cell numbers or demyelination within the spinal cord (figure 9C, D). This finding is in contrast to the results of other studies, which indicate that IL-13 prevents demyelination and thus has neuroprotective properties (74, 81). However, various other factors have to be investigated in order to draw a final conclusion, as astrogliosis, immune cell infiltration and neuroregeneration are all factors which could be responsible for the improvement in functional outcome.

Previous *in vivo* results indicated that IL-13 Mφs could possibly migrate towards the lesion epicenter and thus locally exert anti-inflammatory effects (figure 7C). This migratory capacity is beneficial in suppressing neuroinflammation and stimulating tissue repair, as the Mφs are able to migrate towards the core of neuroinflammation and locally exert anti-inflammatory effects. Therefore, we investigated whether IL-13 Mφs were able to migrate *in vitro* and *in vivo*. To assess *in vitro* migration, we focused on the chemotaxis of these cells towards SDF-1 which is involved in the chemoattraction of blood-borne monocytes/macrophages (91). SDF-1 is an important chemokine involved in the recruitment of many leukocytes and is upregulated after SCI. (92, 93). Unfortunately, we were unable to observe *in vitro* migration of IL-13 Mφs towards the chemokine SDF-1 (figure 10). Optimization of the Boyden chamber assay was performed during this research. However, complete optimization of the concerned technique was not realized. Evaluation of IL-13 Mφ migration did not show consistent results, as an increase in SDF-1 concentration did not alter migration. Therefore, further optimization and experiments focusing on Mφ migration remain necessary to assess the *in vitro* migratory capacity of IL-13 Mφs. In addition, *in vivo* migration of IL-13 Mφs was investigated in mice after SCI. Presence of IL-13 Mφs was determined via the expression of the transduced IL-13 gene and correlated to migration of these cells. Results indicated that IL-13 Mφs were not present at the lesion site at 7dpi (figure 11B). This finding indicates that the IL-13 Mφs were not able to reach the lesion epicenter within the specified time. However, the cells were also not observed within the injection site at 7dpi. This finding illustrates

the possibility of the cells to migrate within the injured spinal cord. Whether these cells are present between the injection and lesion site, or did not survive the experimental conditions, requires further investigation. These results, however, should be interpreted with caution, as further analysis revealed that LV IL-13 primer efficiency was surprisingly low. This is in contrast to the findings in *in vitro* experiments, which showed a high primer efficiency. Yet, in the indicated *in vivo* experiment, the primer efficiency revealed that the obtained results are not reliable. Therefore, a specific conclusion cannot be made and repetition of the concerned experiment with newly designed primers is required. A possible explanation for the deviating primer efficiency in the *in vivo* experiment is the binding of these primers to genes other than the LV IL-13 gene. These genes can be of viral origin, as the primers are complementary to the internal ribosome entry site, related to the viral transcript. This indicates a viral contamination of the spinal cord tissues, either caused *in vivo* or during analysis of the concerned tissues. In addition, we investigated whether the transplantation of IL-13 Mφs resulted in an altered inflammatory state, either within the injection or the lesion site. As previously described, migration of IL-13 Mφs was not observed at 7dpi. However, a bystander effect is still credible in which IL-13 Mφs are able to stimulate M2 polarization of Mφs within the lesion epicenter. This phenomenon can explain the observation of Arg-1^+ Mφs within the lesion site after IL-13 Mφ transplantation. Results showed that, surprisingly, a trend towards a decreased Arg-1 gene expression was observed in the lesion site at 7dpi after IL-13 Mφ transplantation compared to the vehicle group (figure 11C, D). However, it should be mentioned that Arg-1^+ Mφs were observed at 28dpi, while Arg-1 gene expression was assessed at 7dpi. To exactly validate the finding of Arg-1^+ Mφs on gene level, expression of Arg-1 should be further investigated at 28dpi. Further analysis showed no major differences in both anti- and pro-inflammatory gene expression between vehicle- and IL-13 Mφ treated mice. Migration of IL-13 Mφs and the inflammatory state of the spinal cord were investigated at 7dpi. This time period was selected as several studies showed that Mφ infiltration and activation peaks at the 7^{th} day following injury (26, 94). Therefore, we presumed that the migration and anti-inflammatory effects of IL-13 Mφs would be the most prominent at this time period. However, no migration or anti-inflammatory effects were observed. Therefore, other time periods should be included. If IL-13 Mφs do not have the ability to migrate towards the lesion epicenter, further genetic engineering can be performed. Expression of chemokine receptors involved in Mφ migration can be enhanced in order to promote migration of the IL-13 Mφs towards the lesion epicenter. Accordingly, this approach could benefit SCI outcome as the IL-13 Mφs are able to locally exert anti-inflammatory effects at the center of the neuroinflammatory environment.

5 Conclusion

Within this research project, we aimed to investigate the phenotypic properties of IL-13 Mφs and whether these cell improve functional recovery after SCI. Additionally, we evaluated if the IL-13 Mφs have migratory abilities. It is clear that IL-13 induces anti-inflammatory characteristics in Mφs and has been correlated to neuro-protection and –regeneration. Therefore, we hypothesized that IL-13 Mφs improve functional recovery after SCI by locally exerting M2 functions and secreting IL-13.

First, the phenotypic properties of IL-13 Mφs were investigated *in vitro*. This was done both under non-stimulatory and pro-inflammatory conditions. Moreover, we evaluated whether the IL-13 Mφs induced an M2 switch in M1 Mφs. Results demonstrated that IL-13 Mφs had an anti-inflammatory expression profile, similar to M2 Mφs. In fact, a trend towards an increase in anti-inflammatory gene expression was observed in IL-13 Mφs compared to M2 Mφs. Additionally, the IL-13 Mφs were able to maintain this anti-inflammatory expression profile under pro-inflammatory conditions. Moreover, the IL-13 Mφs, and more specific the secretion of these cells, induced an M2 phenotype in both M0 and M1 Mφs, characterized by Arg-1 expression. These *in vitro* results are promising in case of SCI, as the anti-inflammatory characteristics of IL-13 Mφs suppress neuroinflammation, thereby limiting immune-related damage.

Subsequently, the effect of IL-13 Mφs on functional recovery in a spinal cord T-cut hemisection injury mouse model was assessed. As expected, the IL-13 Mφs improved functional recovery after SCI in C57BL/6 mice. Validation of these findings in an IL-4R KO mouse model revealed that IL-13 signaling is essential in the functional improvement regarding IL-13 Mφ transplantation.

Finally, *in vitro* and *in vivo* migration capacity of IL-13 Mφs were evaluated and results indicated no clear migration.

In conclusion, the obtained results do not confirm the stated hypothesis yet. Despite demonstrating anti-inflammatory effects, IL-13 secretion and functional improvement, migration and thus local actions of the IL-13 Mφs were not observed within this research. Therefore, further research is required to elucidate the migratory potential of these cells. Furthermore, future experiments should focus on other beneficial effects in case of SCI. Neuro-protective and –regenerative properties of IL-13 Mφs should be evaluated by performing neurotoxicity assays and neurite outgrowth assays respectively. Moreover, the results of this study contribute to future therapeutic options of SCI. The use of IL-13 Mφs is an interesting approach in the treatment of SCI and can shed light on the ability of genetically engineered cells to treat this devastating condition.

References

1. Jazayeri SB, Beygi S, Shokraneh F, Hagen EM, Rahimi-Movaghar V. Incidence of traumatic spinal cord injury worldwide: a systematic review. European spine journal. 2015;24(5):905-18.
2. Ahuja CS, Wilson JR, Nori S, Kotter MR, Druschel C, Curt A, et al. Traumatic spinal cord injury. Nature Reviews Disease Primers. 2017;3:17018.
3. Winter B, Pattani H, Temple E. Spinal cord injury. Anaesthesia & Intensive Care Medicine. 2017;18(8):404-9.
4. Westgren N, Levi R. Quality of life and traumatic spinal cord injury. Archives of physical medicine and rehabilitation. 1998;79(11):1433-9.
5. North N. The psychological effects of spinal cord injury: a review. Spinal cord. 1999;37(10):671.
6. Haisma J, Van der Woude L, Stam H, Bergen M, Sluis T, Bussmann J. Physical capacity in wheelchair-dependent persons with a spinal cord injury: a critical review of the literature. Spinal cord. 2006;44(11):642.
7. Krueger H, Noonan V, Trenaman L, Joshi P, Rivers C. The economic burden of traumatic spinal cord injury in Canada. Chronic diseases and injuries in Canada. 2013;33(3).
8. Ma VY, Chan L, Carruthers KJ. Incidence, prevalence, costs, and impact on disability of common conditions requiring rehabilitation in the United States: stroke, spinal cord injury, traumatic brain injury, multiple sclerosis, osteoarthritis, rheumatoid arthritis, limb loss, and back pain. Archives of physical medicine and rehabilitation. 2014;95(5):986-95. e1.
9. Baptiste DC, Fehlings MG. Update on the treatment of spinal cord injury. Progress in brain research. 2007;161:217-33.
10. Baptiste DC, Fehlings MG. Pharmacological approaches to repair the injured spinal cord. Journal of neurotrauma. 2006;23(3-4):318-34.
11. Pointillart V, Petitjean M, Wiart L, Vital J, Lassie P, Thicoipé M, et al. Pharmacological therapy of spinal cord injury during the acute phase. Spinal cord. 2000;38(2):71.
12. Ronaghi M, Erceg S, Moreno-Manzano V, Stojkovic M. Challenges of stem cell therapy for spinal cord injury: human embryonic stem cells, endogenous neural stem cells, or induced pluripotent stem cells? Stem cells. 2010;28(1):93-9.
13. Dumont RJ, Okonkwo DO, Verma S, Hurlbert RJ, Boulos PT, Ellegala DB, et al. Acute spinal cord injury, part I: pathophysiologic mechanisms. Clinical neuropharmacology. 2001;24(5):254-64.
14. Tator CH. Update on the pathophysiology and pathology of acute spinal cord injury. Brain pathology. 1995;5(4):407-13.
15. Mautes AE, Weinzierl MR, Donovan F, Noble LJ. Vascular events after spinal cord injury: contribution to secondary pathogenesis. Physical therapy. 2000;80(7):673-87.
16. Oyinbo CA. Secondary injury mechanisms in traumatic spinal cord injury: a nugget of this multiply cascade. Acta Neurobiol Exp (Wars). 2011;71(2):281-99.
17. David S, Kroner A, Greenhalgh AD, Zarruk JG, López-Vales R. Myeloid cell responses after spinal cord injury. Journal of neuroimmunology. 2018.
18. David S, Kroner A. Repertoire of microglial and macrophage responses after spinal cord injury. Nature Reviews Neuroscience. 2011;12(7):388.
19. Means ED, Anderson DK. Neuronophagia by leukocytes in experimental spinal cord injury. Journal of Neuropathology & Experimental Neurology. 1983;42(6):707-19.
20. Sroga JM, Jones TB, Kigerl KA, McGaughy VM, Popovich PG. Rats and mice exhibit distinct inflammatory reactions after spinal cord injury. Journal of Comparative Neurology. 2003;462(2):223-40.
21. Pineau I, Lacroix S. Proinflammatory cytokine synthesis in the injured mouse spinal cord: multiphasic expression pattern and identification of the cell types involved. Journal of Comparative Neurology. 2007;500(2):267-85.
22. Blight A. Macrophages and inflammatory damage in spinal cord injury. Journal of neurotrauma. 1992;9:S83-91.
23. BLIGHT AR. Delayed demyelination and macrophage invasion: a candidate for secondary cell damage in spinal cord injury. Central Nervous System Trauma. 1985;2(4):299-315.
24. Redford E, Kapoor R, Smith K. Nitric oxide donors reversibly block axonal conduction: demyelinated axons are especially susceptible. Brain: a journal of neurology. 1997;120(12):2149-57.
25. Fitch MT, Silver J. Glial cell extracellular matrix: boundaries for axon growth in development and regeneration. Cell and tissue research. 1997;290(2):379-84.
26. Popovich PG, Wei P, Stokes BT. Cellular inflammatory response after spinal cord injury in Sprague-Dawley and Lewis rats. Journal of comparative neurology. 1997;377(3):443-64.

27. Faulkner JR, Herrmann JE, Woo MJ, Tansey KE, Doan NB, Sofroniew MV. Reactive astrocytes protect tissue and preserve function after spinal cord injury. Journal of Neuroscience. 2004;24(9):2143-55.
28. Karimi-Abdolrezaee S, Billakanti R. Reactive astrogliosis after spinal cord injury—beneficial and detrimental effects. Molecular neurobiology. 2012;46(2):251-64.
29. Yiu G, He Z. Glial inhibition of CNS axon regeneration. Nature Reviews Neuroscience. 2006;7(8):617.
30. Fitch MT, Silver J. CNS injury, glial scars, and inflammation: Inhibitory extracellular matrices and regeneration failure. Experimental neurology. 2008;209(2):294-301.
31. O'Shea TM, Burda JE, Sofroniew MV. Cell biology of spinal cord injury and repair. The Journal of clinical investigation. 2017;127(9):3259-70.
32. Rice T, Larsen J, Rivest S, Yong VW. Characterization of the early neuroinflammation after spinal cord injury in mice. Journal of Neuropathology & Experimental Neurology. 2007;66(3):184-95.
33. Fleming JC, Norenberg MD, Ramsay DA, Dekaban GA, Marcillo AE, Saenz AD, et al. The cellular inflammatory response in human spinal cords after injury. Brain. 2006;129(12):3249-69.
34. Ahmed A, Patil A-A, Agrawal DK. Immunobiology of spinal cord injuries and potential therapeutic approaches. Molecular and cellular biochemistry. 2018;441(1-2):181-9.
35. Ley K, Laudanna C, Cybulsky MI, Nourshargh S. Getting to the site of inflammation: the leukocyte adhesion cascade updated. Nature Reviews Immunology. 2007;7(9):678.
36. Tysseling VM, Mithal D, Sahni V, Birch D, Jung H, Miller RJ, et al. SDF1 in the dorsal corticospinal tract promotes CXCR4+ cell migration after spinal cord injury. Journal of neuroinflammation. 2011;8(1):16.
37. Mabon PJ, Weaver LC, Dekaban GA. Inhibition of monocyte/macrophage migration to a spinal cord injury site by an antibody to the integrin αD: a potential new anti-inflammatory treatment. Experimental neurology. 2000;166(1):52-64.
38. Schwab JM, Zhang Y, Kopp MA, Brommer B, Popovich PG. The paradox of chronic neuroinflammation, systemic immune suppression, autoimmunity after traumatic chronic spinal cord injury. Experimental neurology. 2014;258:121-9.
39. Donnelly DJ, Popovich PG. Inflammation and its role in neuroprotection, axonal regeneration and functional recovery after spinal cord injury. Experimental neurology. 2008;209(2):378-88.
40. Perry V, Brown M. Role of macrophages in peripheral nerve degeneration and repair. Bioessays. 1992;14(6):401-6.
41. Hausmann O. Post-traumatic inflammation following spinal cord injury. Spinal cord. 2003;41(7):369.
42. Ren Y, Young W. Managing inflammation after spinal cord injury through manipulation of macrophage function. Neural plasticity. 2013;2013.
43. Prüss H, Kopp MA, Brommer B, Gatzemeier N, Laginha I, Dirnagl U, et al. Non-resolving aspects of acute inflammation after spinal cord injury (SCI): Indices and resolution plateau. Brain pathology. 2011;21(6):652-60.
44. Zhu Y, Soderblom C, Krishnan V, Ashbaugh J, Bethea J, Lee J. Hematogenous macrophage depletion reduces the fibrotic scar and increases axonal growth after spinal cord injury. Neurobiology of disease. 2015;74:114-25.
45. Francos-Quijorna I, Amo-Aparicio J, Martinez-Muriana A, López-Vales R. IL-4 drives microglia and macrophages toward a phenotype conducive for tissue repair and functional recovery after spinal cord injury. Glia. 2016;64(12):2079-92.
46. Norden DM, Faw TD, McKim DB, Deibert RJ, Fisher LC, Sheridan JF, et al. Bone Marrow-Derived Monocytes Drive the Inflammatory Microenvironment in Local and Remote Regions after Thoracic Spinal Cord Injury. Journal of neurotrauma. 2019;36(6):937-49.
47. Gensel JC, Zhang B. Macrophage activation and its role in repair and pathology after spinal cord injury. Brain research. 2015;1619:1-11.
48. Haan N, Zhu B, Wang J, Wei X, Song B. Crosstalk between macrophages and astrocytes affects proliferation, reactive phenotype and inflammatory response, suggesting a role during reactive gliosis following spinal cord injury. Journal of neuroinflammation. 2015;12(1):109.
49. Martinez FO, Sica A, Mantovani A, Locati M. Macrophage activation and polarization. Front Biosci. 2008;13(1):453-61.
50. Kigerl KA, Gensel JC, Ankeny DP, Alexander JK, Donnelly DJ, Popovich PG. Identification of two distinct macrophage subsets with divergent effects causing either neurotoxicity or regeneration in the injured mouse spinal cord. Journal of Neuroscience. 2009;29(43):13435-44.

51. Kumar A, Alvarez-Croda D-M, Stoica BA, Faden AI, Loane DJ. Microglial/macrophage polarization dynamics following traumatic brain injury. Journal of neurotrauma. 2016;33(19):1732-50.
52. Faden AI, Wu J, Stoica BA, Loane DJ. Progressive inflammation-mediated neurodegeneration after traumatic brain or spinal cord injury. British journal of pharmacology. 2016;173(4):681-91.
53. Popovich PG, Guan Z, Wei P, Huitinga I, van Rooijen N, Stokes BT. Depletion of hematogenous macrophages promotes partial hindlimb recovery and neuroanatomical repair after experimental spinal cord injury. Experimental neurology. 1999;158(2):351-65.
54. Gris D, Marsh DR, Oatway MA, Chen Y, Hamilton EF, Dekaban GA, et al. Transient blockade of the CD11d/CD18 integrin reduces secondary damage after spinal cord injury, improving sensory, autonomic, and motor function. Journal of Neuroscience. 2004;24(16):4043-51.
55. Ma S-F, Chen Y-J, Zhang J-X, Shen L, Wang R, Zhou J-S, et al. Adoptive transfer of M2 macrophages promotes locomotor recovery in adult rats after spinal cord injury. Brain, behavior, and immunity. 2015;45:157-70.
56. Jiang MH, Chung E, Chi GF, Ahn W, Lim JE, Hong HS, et al. Substance P induces M2-type macrophages after spinal cord injury. Neuroreport. 2012;23(13):786-92.
57. Zhou Z, Peng X, Insolera R, Fink DJ, Mata M. IL-10 promotes neuronal survival following spinal cord injury. Experimental neurology. 2009;220(1):183-90.
58. Mantovani A, Biswas SK, Galdiero MR, Sica A, Locati M. Macrophage plasticity and polarization in tissue repair and remodelling. The Journal of pathology. 2013;229(2):176-85.
59. Sindrilaru A, Peters T, Wieschalka S, Baican C, Baican A, Peter H, et al. An unrestrained proinflammatory M1 macrophage population induced by iron impairs wound healing in humans and mice. The Journal of clinical investigation. 2011;121(3):985-97.
60. Kong X, Gao J. Macrophage polarization: a key event in the secondary phase of acute spinal cord injury. Journal of cellular and molecular medicine. 2017;21(5):941-54.
61. Burd P, Thompson W, Max E, Mills F. Activated mast cells produce interleukin 13. Journal of Experimental Medicine. 1995;181(4):1373-80.
62. Li H, Sim TC, Alam R. IL-13 released by and localized in human basophils. The Journal of Immunology. 1996;156(12):4833-8.
63. McKenzie A, Culpepper J, de Waal Malefyt R, Briere F, Punnonen J, Aversa G, et al. Interleukin 13, a T-cell-derived cytokine that regulates human monocyte and B-cell function. Proceedings of the National Academy of Sciences. 1993;90(8):3735-9.
64. Minty A, Chalon P, Derocq J-M, Dumont X, Guillemot J-C, Kaghad M, et al. Interleukin-13 is a new human lymphokine regulating inflammatory and immune responses. Nature. 1993;362(6417):248.
65. Kelly-Welch AE, Hanson EM, Boothby MR, Keegan AD. Interleukin-4 and interleukin-13 signaling connections maps. Science. 2003;300(5625):1527-8.
66. Le Blon D, Guglielmetti C, Hoornaert C, Quarta A, Daans J, Dooley D, et al. Intracerebral transplantation of interleukin 13-producing mesenchymal stem cells limits microgliosis, oligodendrocyte loss and demyelination in the cuprizone mouse model. Journal of neuroinflammation. 2016;13(1):288.
67. Kawahara K, Suenobu M, Yoshida A, Koga K, Hyodo A, Ohtsuka H, et al. Intracerebral microinjection of interleukin-4/interleukin-13 reduces β-amyloid accumulation in the ipsilateral side and improves cognitive deficits in young amyloid precursor protein 23 mice. Neuroscience. 2012;207:243-60.
68. Wills-Karp M, Luyimbazi J, Xu X, Schofield B, Neben TY, Karp CL, et al. Interleukin-13: central mediator of allergic asthma. Science. 1998;282(5397):2258-61.
69. Pierigè F, Serafini S, Rossi L, Magnani M. Cell-based drug delivery. Advanced drug delivery reviews. 2008;60(2):286-95.
70. Geurts N, Vangansewinkel T, Lemmens S, Nelissen S, Geboes L, Schwartz C, et al. Basophils are dispensable for the recovery of gross locomotion after spinal cord hemisection injury. Journal of leukocyte biology. 2016;99(4):579-82.
71. Dooley D, Lemmens E, Vangansewinkel T, Le Blon D, Hoornaert C, Ponsaerts P, et al. Cell-based delivery of interleukin-13 directs alternative activation of macrophages resulting in improved functional outcome after spinal cord injury. Stem cell reports. 2016;7(6):1099-115.
72. Miron VE, Boyd A, Zhao J-W, Yuen TJ, Ruckh JM, Shadrach JL, et al. M2 microglia and macrophages drive oligodendrocyte differentiation during CNS remyelination. Nature neuroscience. 2013;16(9):1211.

73. Shin WH, Lee DY, Park KW, Kim SU, Yang MS, Joe EH, et al. Microglia expressing interleukin-13 undergo cell death and contribute to neuronal survival in vivo. Glia. 2004;46(2):142-52.
74. Guglielmetti C, Le Blon D, Santermans E, Salas-Perdomo A, Daans J, De Vocht N, et al. Interleukin-13 immune gene therapy prevents CNS inflammation and demyelination via alternative activation of microglia and macrophages. Glia. 2016;64(12):2181-200.
75. Sica A, Mantovani A. Macrophage plasticity and polarization: in vivo veritas. The Journal of clinical investigation. 2012;122(3):787-95.
76. Tugal D, Liao X, Jain MK. Transcriptional control of macrophage polarization. Arteriosclerosis, thrombosis, and vascular biology. 2013;33(6):1135-44.
77. Boehler R, Kuo R, Shin S, Goodman A, Pilecki M, Leonard JN, et al. Lentivirus delivery of IL-10 to promote and sustain macrophage polarization towards an anti-inflammatory phenotype. Biotechnology and bioengineering. 2014;111(6):1210-21.
78. Fenn AM, Hall JC, Gensel JC, Popovich PG, Godbout JP. IL-4 signaling drives a unique arginase+/IL-1β+ microglia phenotype and recruits macrophages to the inflammatory CNS: consequences of age-related deficits in IL-4Rα after traumatic spinal cord injury. Journal of Neuroscience. 2014;34(26):8904-17.
79. Smith TD, Tse MJ, Read EL, Liu WF. Regulation of macrophage polarization and plasticity by complex activation signals. Integrative Biology. 2016;8(9):946-55.
80. Sinha P, Clements VK, Ostrand-Rosenberg S. Interleukin-13–regulated M2 macrophages in combination with myeloid suppressor cells block immune surveillance against metastasis. Cancer research. 2005;65(24):11743-51.
81. Dooley D, Lemmens E, Vangansewinkel T, Lemmens S, De Vocht N, Le Blon D, et al. Mesenchymal stem cells overexpressing IL-13 decrease lesion size and demyelination after spinal cord injury. Journal of Neuroimmunology. 2014;275(1):160.
82. Nakajima H, Uchida K, Guerrero AR, Watanabe S, Sugita D, Takeura N, et al. Transplantation of mesenchymal stem cells promotes an alternative pathway of macrophage activation and functional recovery after spinal cord injury. Journal of neurotrauma. 2012;29(8):1614-25.
83. Urdzíková L, Růžička J, LaBagnara M, Kárová K, Kubinová Š, Jiráková K, et al. Human mesenchymal stem cells modulate inflammatory cytokines after spinal cord injury in rat. International journal of molecular sciences. 2014;15(7):11275-93.
84. Abrams MB, Dominguez C, Pernold K, Reger R, Wiesenfeld-Hallin Z, Olson L, et al. Multipotent mesenchymal stromal cells attenuate chronic inflammation and injury-induced sensitivity to mechanical stimuli in experimental spinal cord injury. Restorative neurology and neuroscience. 2009;27(4):307-21.
85. Qu J, Zhang H. Roles of mesenchymal stem cells in spinal cord injury. Stem cells international. 2017;2017.
86. Zurawski SM, Vega Jr F, Huyghe B, Zurawski G. Receptors for interleukin-13 and interleukin-4 are complex and share a novel component that functions in signal transduction. The EMBO journal. 1993;12(7):2663-70.
87. Gordon S. Alternative activation of macrophages. Nature reviews immunology. 2003;3(1):23.
88. LEMMENS E, VIDAL VERA P, NELISSEN S, VANGANSEWINKEL T, HENDRIX S, editors. INTERLEUKIN-13 STIMULATES NEURITE OUTGROWTH IN VITRO IN PRIMARY NEURONS AND ORGANOTYPIC BRAIN SLICES WHILE IT WORSENS CLINICAL OUTCOME AFTER SPINAL CORD INJURY IN VIVO2011: WILEY-BLACKWELL.
89. Basso DM, Fisher LC, Anderson AJ, Jakeman LB, Mctigue DM, Popovich PG. Basso Mouse Scale for locomotion detects differences in recovery after spinal cord injury in five common mouse strains. Journal of neurotrauma. 2006;23(5):635-59.
90. Sellers R, Clifford C, Treuting P, Brayton C. Immunological variation between inbred laboratory mouse strains: points to consider in phenotyping genetically immunomodified mice. Veterinary pathology. 2012;49(1):32-43.
91. Fernandez EJ, Lolis E. Structure, function, and inhibition of chemokines. Annual review of pharmacology and toxicology. 2002;42(1):469-99.
92. Bartholdi D, Schwab ME. Expression of pro-inflammatory cytokine and chemokine mRNA upon experimental spinal cord injury in mouse: An in situ hybridization study. European Journal of Neuroscience. 1997;9(7):1422-38.
93. Jaerve A, Bosse F, Müller HW. SDF-1/CXCL12: its role in spinal cord injury. The international journal of biochemistry & cell biology. 2012;44(3):452-6.
94. Dusart I, Schwab M. Secondary cell death and the inflammatory reaction after dorsal hemisection of the rat spinal cord. European Journal of Neuroscience. 1994;6(5):712-24.

Appendix

Table A1: Primers used within this research.

Gene	Primer sequence	
	Forward 5′-3′	*Reverse 5′-3′*
Arg-1	*GTGAAGAACCCACGGTCTGT*	*GCCAGAGATGCTTCCAACTG*
CD38	*ACTGGAGAGCCTACCACGAA*	*TGGGCCAGGTGTTTGGATTT*
CD86	*GAGCGGGATAGTAACGCTGA*	*GGCTCTCACTGCCTTCACTC*
CD206	*CTTCGGGCCTTTGGAATAAT*	*TAGAAGAGCCCTTGGGTTGA*
CycA	*GCGTCTCCTTCGAGCTGTT*	*AAGTCACCACCCTGGCA*
Fizz	*TCCAGCTAACTATCCCTCCACTGT*	*GGCCCATCTGTTCATAGTCTTGA*
GAPDH	*GGCCTTCCGTGTTCCTAC*	*TGTCATCATATCTGGCAGGTT*
HMBS	*GATGGGCAACTGTACCTGACTG*	*CTGGGCTCCTCTTGGAATG*
iNOS	*CCCTTCAATGGTTGGTACATGG*	*ACATTGATCTCCGTGACAGCC*
LV IL-13	*GAAGCCGCTTGGAATAAGGC*	*ACCTTGCATTCCTTTGGCGA*
MHC-II	*GCTCTCGGAGACCTATGACG*	*ACAGGCAAACCTCTGGACAC*
TNFα	*GTCCCCAAAGGGATGAGAAGT*	*TTTGCTACGACGTGGGCTAC*
Ym1	*GGGCATACCTTTATCCTGAG*	*CCACTGAAGTCATCCATGTC*
YWHAZ	*GCAACGATGTACTGTCTCTTTTGG*	*GTCCACAATTCCTTTCTTGTCATC*

Arg-1, arginase-1; CD38, cluster of differentiation 38; CD86, cluster of differentiation 86; CD206, mannose receptor; CycA, Cyclin A; Fizz, resistin like alpha; GAPDH, glyceraldehyde 3-phosphate dehydrogenase; HMBS, hydroxymethylbilane synthase; iNOS, inducible nitric oxide synthase; LV IL-13, lentiviral interleukin-13; MHC-II, major histocompatibility complex class II; TNFα, tumor necrosis factor alpha; Ym1, chitinase 3-like 3; YWHAZ, 14-3-3 protein zeta/delta.

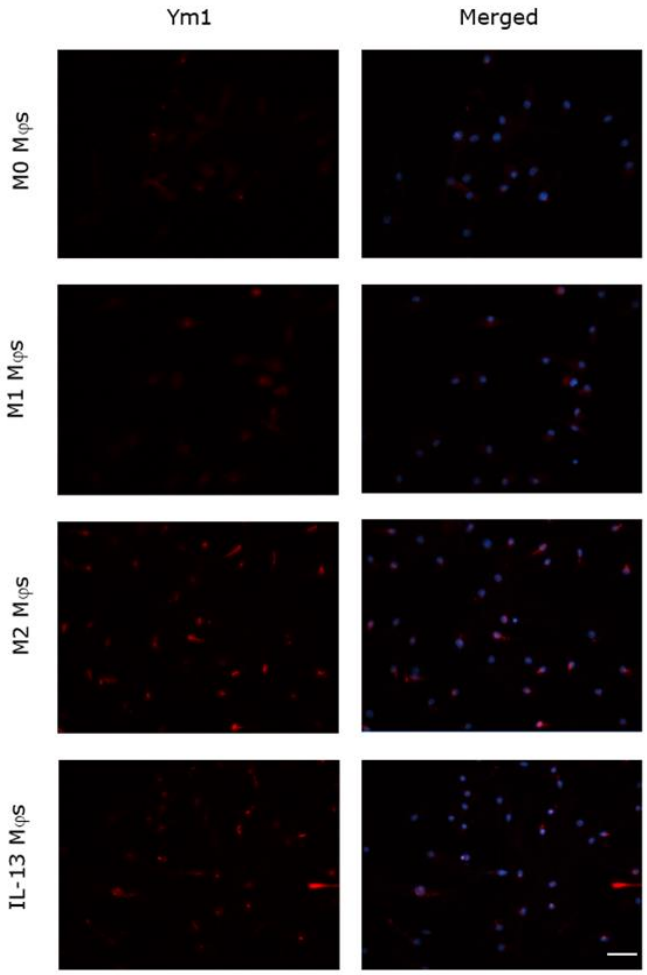

Figure A1: Ym1 expression is increased in IL-13 Mφs. BMDMs were either left unstimulated or were stimulated with 100 ng/mL LPS or 33.3 ng/mL rIL-13 for 24h and 48h respectively to obtain M0, M1, and M2 Mφs. IL-13 Mφs were obtained by transducing BMDMs with lentiviral vectors containing murine IL-13 cDNA. Ym1 expression was investigated by histological analysis. n=1. *BMDMs, bone marrow-derived macrophages; LPS, lipopolysaccharide; IL-13, interleukin-13; Mφs, macrophages; Ym1, chitinase 3-like 3.*

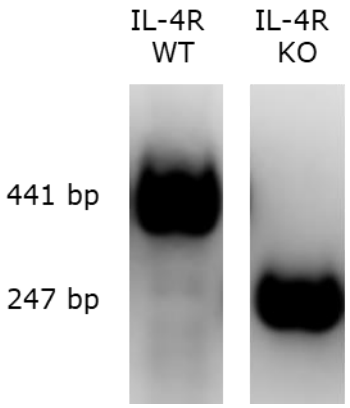

Figure A2: Genotyping of IL-4R WT and KO mice. DNA fragments were assessed for KO of the IL-4R gene. Presence of DNA fragments of 247 bp indicated functional KO of the concerned gene. *bp, base pairs; IL-4R, interleukin-4 receptor; KO, knockout; WT, wild type.*